

# A computable branching process for the Wigner quantum dynamics

Sihong Shao<sup>†</sup>      Yunfeng Xiong<sup>†</sup>

September 30, 2022

## Abstract

A branching process treatment for the nonlocal Wigner pseudo-differential operator and its numerical applications in quantum dynamics is proposed and analyzed. We start from the discussion on two typical truncations of the non-local term, i.e., the  $k$ -truncated and  $y$ -truncated models. After introducing an auxiliary function  $\gamma(\mathbf{x})$ , the (truncated) Wigner equation is reformulated into the integral formulation as well as its adjoint correspondence, both of which can be regarded as the renewal-type equations and have transparent stochastic interpretation. We prove that the moment of a branching process happens to be the solution for the adjoint equation, which connects rigorously the Wigner quantum dynamics to the stochastic branching process, and thus a sound mathematical framework for the Wigner Monte Carlo methods is established. Within the framework, the branching process for the  $y$ -truncated model recovers the popular signed particle Monte Carlo method which needs a discretization of the momentum space beforehand, whereas the  $k$ -truncated branching method allows a continuous momentum sampling. More interestingly, with the help of the rigorous connection, we find that a constant auxiliary function  $\gamma(\mathbf{x}) \equiv \gamma_0$  performs better from the point of view of both theoretical and numerical aspects. In theory, we obtain a simple but analytical calculation formula for the growth rate of particle number, i.e.,  $e^{2\gamma_0 t}$  with  $t$  being the time. In numerics, the constant auxiliary function may facilitate the random sampling from the exponential distribution and improve the accuracy. Typical numerical experiments on the Gaussian barrier scattering validate our theoretical findings, as well as demonstrate the accuracy, the efficiency and thus the computability of the Wigner branching process.

**Keywords:** Wigner equation; branching process; quantum dynamics; adjoint equation; renewal-type integral equations; importance sampling; signed particle Monte Carlo method; Gaussian barrier scattering

---

<sup>†</sup>LMAM and School of Mathematical Sciences, Peking University, Beijing 100871, China.

# 1 Introduction

Connections between partial differential equations (PDE) and stochastic processes are always heated topics in modern mathematics and provide powerful tools for both probability theory and analysis, especially for PDE of elliptic and parabolic type [1,2]. In the past few decades, their numerical applications have also burgeoned with a lot of developments, such as the iterative Monte Carlo method for the Boltzmann transport equation [3], the random walk method for the Laplace equation [4] and the diffusion Monte Carlo method for the Schrödinger equation [5]. In particular, the diffusion Monte Carlo method allows us to go beyond the mean-field approximation and offer a direct, reliable solution to quantum many-body systems. In this work, we focus on the probabilistic approach to the equivalent phase space formalism of quantum mechanics, namely, the Wigner function approach [6], which bears a close analogy to classical mechanics and has been drawing growing attention [7–10]. In recent years, the Wigner equation has been widely used in nanoelectronics [11,12], non-equilibrium statistical mechanics [13], quantum optics [14], and many-body quantum systems [15]. Actually, a branch of experiment physics in the community of quantum tomography are devoting to reconstructing the Wigner function from measurements [16,17]. Moreover, the intriguing mathematical structure of the Wigner equation has also been employed in the deformation quantization [18].

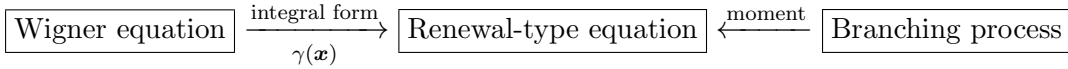
Despite its theoretical advantages, solving the Wigner equation is extremely problematic, because of the high dimensionality of the phase space, as well as the highly oscillating structure of the Wigner function due to the spatial coherence [8,17]. Although an efficient deterministic method, i.e., the conservative spectral element method (SEM), has enabled an accurate transient simulation, it is still confined to the one-dimensional one-body case [19]. It is not until recently have the authors made the first attempt to solve the one-dimensional two-body problem through a third-order advection-spectral-mixed scheme [20]. By contrast, stochastic methods representing the (quasi-) distribution by finite number of super-particles, can significantly reduce the requirement for data storage for high dimensional simulations, and provide satisfactory, albeit less accurate numerical solutions [21–23]. More importantly, they allow an easier fashion for parallelization in modern high performance computing platforms, thereby facilitating their applications in quantum many-body systems [15]. Up to now, there mainly exists three particle-based stochastic approaches for the Wigner simulations in the literature [21,22].

The first approach, called the ensemble Wigner Monte Carlo method, is a generalization of classical Boltzmann transport simulations and each particle is endowed with an additional particle affinity to carry the quantum information [24–26]. This method is applicable for simulating one-dimensional resonant tunneling diode, but suffers from the increasing computational complexity while regarding the high dimensional affinity evolution [21]. The second approach, designed for the stationary Wigner-Boltzmann equation associated with a specified boundary condition, is to exploit the ergodicity of the trajectories, so that the physical average can be obtained through a time average over a single particle. This yields a single particle Monte Carlo method, with the branching of signed particles to manifest the quantum ef-

fect [27]. As two major ingredients of the second method, both the dual system of the Wigner equation and the branching process also play a vital role in the third approach, called the signed particle Wigner Monte Carlo (spWMC) method [22, 28]. This approach utilizes the same idea of particle branching to capture the quantum coherence, and has also proven to be a promising tool for many-body Wigner simulations [15].

Although the spWMC method has been found to be effective and may probably overcome the computational burden in fully quantum many-body simulations, to the extent of our knowledge, there has been so far no detailed mathematical analysis about it. Only recently, its numerical accuracy for one-dimensional one-body problem has been validated by comparing with SEM, whereas its stability as well as the applicability range remain unclear [23]. To this end, this work makes a further step towards the construction of firm mathematical foundations for spWMC, and explores the inherent relation between the Wigner equation and the stochastic process. Only by this can we thoroughly understand the underlying idea and make further improvements on related numerical algorithms.

The main purpose of this paper is twofold. First, we would like to dig out the inherent connection between the Wigner equation and a stochastic branching process, which can be sketched by the diagram below.



By introducing an auxiliary function  $\gamma(\mathbf{x})$ , we are able to cast both the Wigner equation and its adjoint equation into the renewal-type equations, whose solution can be interpreted as the first moment of a stochastic branching process. In this manner, we arrive at the stochastic interpretation of the Wigner quantum dynamics, termed the *Wigner branching process* in this work. It provides us not only an intuition, but also a rigorous mathematical tool to study the Wigner equation. Furthermore, based on the principle of importance sampling, such a probabilistic approach allows us to calculate macroscopically measurable quantities, including the Wigner function itself, by simply tracking the trajectories of signed super-particles. One possible drawback of this method lies in the exponential growth of the particle number in a branching system, putting the data storage extremely demanding. Fortunately, this problem can be alleviated by exploiting the dual system of the Wigner equation (the adjoint equation), which facilitates the use of the Markovian property of the evolution system and permits us to annihilate the redundant particles through the resampling procedure at a prescribed frequency.

The spWMC method is just a special case of the Wigner branching process and might not be the best choice for many-body problems. Thus, our second goal is to promote its reliability and applicability range. We propose a branching particle system in which each particle carries a weight ranging in  $[-1, 1]$ , instead of only in  $\{-1, 1\}$  within spWMC, and its lifetime is characterized by an exponential distribution with a constant parameter  $\gamma_0$ . Such constant auxiliary function  $\gamma(\mathbf{x}) \equiv \gamma_0$  not only improves the accuracy of the stochastic method, but also facilitates the estimate on the growth rate of particle number. In fact, we derive an exact calcula-

tion formula for the growth rate of particle number which reads  $e^{2\gamma_0 t}$  with  $t$  being the time. In addition, we will show the necessity and feasibility of sampling in the continuous  $\mathbf{k}$ -space (i.e., the proposed  $k$ -truncated model), and point out the latent weakness of the semi-discrete model (or termed the  $y$ -truncated model in this work).

The rest of this paper is organized as follows. Section 2 reviews briefly the Wigner formalism of quantum mechanics. From numerical aspects, we are only able to solve the truncated Wigner equation, instead of the Wigner equation itself. Thus in Section 3, we illustrate two typical ways to truncate the Wigner equation, termed the  $k$ -truncated and the  $y$ -truncated models. Section 4 manifests the equivalence between the  $k$ -truncated Wigner model and a renewal-type integral equation, where an auxiliary function  $\gamma(\mathbf{x})$  is used to introduce a probability measure in its formulation. Besides, the set of adjoint equation renders an equivalent representation of the inner product problem. In Section 5, we will show that such representation, as well as the importance sampling, plays a vital role in the Wigner Monte Carlo method and motivates us to discuss the Wigner branching process, namely, there exists a branching process associated with an exit measure such that its first moment is exactly the solution of the adjoint equation. This probabilistic approach not only validates the branching process treatment, but also allows us to study the mass conservation and growth of particle number rigorously. In Section 6, we turn to discuss several numerical treatments in implementing the Wigner branching process. Section 7 investigates the performance of the proposed stochastic methods by employing SEM as the reference. The paper is concluded in Section 8 with a few open discussions.

## 2 The Wigner equation

In this section, we briefly review the Wigner representation of quantum mechanics. The Wigner function  $f(\mathbf{x}, \mathbf{k}, t)$  living in the phase space  $(\mathbf{x}, \mathbf{k}) \in \mathbb{R}^{2d}$  for position  $\mathbf{x}$  and wavevector  $\mathbf{k}$ ,

$$f(\mathbf{x}, \mathbf{k}, t) = \int_{\mathbb{R}^d} d\mathbf{y} \, e^{-i\mathbf{k} \cdot \mathbf{y}} \rho(\mathbf{x} + \frac{\mathbf{y}}{2}, \mathbf{x} - \frac{\mathbf{y}}{2}, t), \quad (1)$$

is defined by the Weyl-Wigner transform of the density matrix

$$\rho(\mathbf{x}_1, \mathbf{x}_2, t) = \sum_i p_i \Psi_i(\mathbf{x}_1, t) \Psi_i^\dagger(\mathbf{x}_2, t), \quad (2)$$

where  $p_i$  gives the probability of occupying the  $i$ -th state,  $2d$  denotes the degree of freedom ( $2 \times \text{particle number} \times \text{dimensionality}$ ). Although *it allows possible negative values*, the Wigner function serves the role as a distribution due to the following properties [7, 9]

- $f(\mathbf{x}, \mathbf{k}, t)$  is a real function.
- $\iint_{\mathbb{R}^d \times \mathbb{R}^d} f(\mathbf{x}, \mathbf{k}, t) d\mathbf{x} d\mathbf{k} = 1$ .

- The average of any function  $A(\mathbf{x}, \mathbf{k})$  can be written in a form

$$\langle A \rangle_t = \iint_{\mathbb{R}^d \times \mathbb{R}^d} A(\mathbf{x}, \mathbf{k}) f(\mathbf{x}, \mathbf{k}, t) d\mathbf{x} d\mathbf{k}. \quad (3)$$

In particular, by taking  $A(\mathbf{x}, \mathbf{k})$  as an indicator function  $1_D(\mathbf{x}, \mathbf{k})$  on a given phase space domain  $D$ , we obtain the *Wigner (quasi-) probability* on  $D$  as follows

$$\langle 1_D \rangle_t = \iint_D f(\mathbf{x}, \mathbf{k}, t) d\mathbf{x} d\mathbf{k}. \quad (4)$$

To derive the dynamics of the Wigner function, we evaluate its first derivative through the Schrödinger equation (or the quantum Liouville equation)

$$\mathbf{i}\hbar \frac{\partial}{\partial t} \Psi_i(\mathbf{x}, t) = -\frac{\hbar^2}{2m} \nabla_{\mathbf{x}}^2 \Psi_i(\mathbf{x}, t) + V(\mathbf{x}, t) \Psi_i(\mathbf{x}, t), \quad (5)$$

combine with the Fourier completeness relation

$$\delta(\mathbf{k}' - \mathbf{k}) = \frac{1}{(2\pi)^d} \int_{\mathbb{R}^d} d\mathbf{y} e^{\mathbf{i}(\mathbf{k} - \mathbf{k}') \cdot \mathbf{y}}, \quad (6)$$

and then obtain the Wigner equation

$$\frac{\partial}{\partial t} f(\mathbf{x}, \mathbf{k}, t) + \frac{\hbar \mathbf{k}}{m} \cdot \nabla_{\mathbf{x}} f(\mathbf{x}, \mathbf{k}, t) = \Theta_V[f](\mathbf{x}, \mathbf{k}, t), \quad (7)$$

where

$$\Theta_V[f](\mathbf{x}, \mathbf{k}, t) = \int_{\mathbb{R}^d} d\mathbf{k}' f(\mathbf{x}, \mathbf{k}', t) V_w(\mathbf{x}, \mathbf{k} - \mathbf{k}', t), \quad (8)$$

$$V_w(\mathbf{x}, \mathbf{k}, t) = \frac{1}{\mathbf{i}\hbar(2\pi)^d} \int_{\mathbb{R}^d} d\mathbf{y} e^{-\mathbf{i}\mathbf{k} \cdot \mathbf{y}} D_V(\mathbf{x}, \mathbf{y}, t), \quad (9)$$

$$D_V(\mathbf{x}, \mathbf{y}, t) = V(\mathbf{x} + \frac{\mathbf{y}}{2}, t) - V(\mathbf{x} - \frac{\mathbf{y}}{2}, t). \quad (10)$$

Here the nonlocal pseudo-differential term  $\Theta_V[f](\mathbf{x}, \mathbf{k}, t)$  contains the quantum information,  $D_V(\mathbf{x}, \mathbf{y}, t)$  denotes a central difference of the potential function  $V(\mathbf{x}, t)$ , the Wigner kernel  $V_w(\mathbf{x}, \mathbf{k}, t)$  is defined through the Fourier transform of  $D_V(\mathbf{x}, \mathbf{y}, t)$ ,  $\hbar$  is the reduced Planck constant and  $m$  is the particle mass (for simplicity, we assume all particles have the same mass throughout this work). Equivalently, we can first perform the integration in  $\mathbf{k}'$ -space and arrive at another way to formulate the pseudo-differential term

$$\Theta_V[f](\mathbf{x}, \mathbf{k}, t) = \frac{1}{\mathbf{i}\hbar} \int_{\mathbb{R}^d} d\mathbf{y} D_V(\mathbf{x}, \mathbf{y}, t) \widehat{f}(\mathbf{x}, \mathbf{y}, t) e^{-\mathbf{i}\mathbf{k} \cdot \mathbf{y}}, \quad (11)$$

$$\widehat{f}(\mathbf{x}, \mathbf{y}, t) = \frac{1}{(2\pi)^d} \int_{\mathbb{R}^d} d\mathbf{k}' f(\mathbf{x}, \mathbf{k}', t) e^{\mathbf{i}\mathbf{k}' \cdot \mathbf{y}} := \mathcal{F}^{-1}[f](\mathbf{x}, \mathbf{y}, t). \quad (12)$$

Actually,  $\widehat{f}(\mathbf{x}, \mathbf{y}, t)$  is just another notation for  $\rho(\mathbf{x} + \frac{\mathbf{y}}{2}, \mathbf{x} - \frac{\mathbf{y}}{2}, t)$ .

One of the most important properties of the Wigner equation lies in the anti-symmetry of the Wigner kernel

$$V_w(\mathbf{x}, \mathbf{k}, t) = -V_w(\mathbf{x}, -\mathbf{k}, t), \quad (13)$$

then a simple calculation yields

$$\int_{\mathbb{R}^d} d\mathbf{k} \int_{\mathbb{R}^d} d\mathbf{k}' f(\mathbf{x}, \mathbf{k}', t) V_w(\mathbf{x}, \mathbf{k} - \mathbf{k}', t) = 0, \quad (14)$$

which corresponds to the conservation of the first moment (i.e., total particle number or mass)

$$\frac{d}{dt} \iint_{\mathbb{R}^d \times \mathbb{R}^d} f(\mathbf{x}, \mathbf{k}, t) d\mathbf{x} d\mathbf{k} = 0. \quad (15)$$

Although the Wigner equation is formally (completely) equivalent to the Schrödinger equation in the full space, we would like to point out that such an equivalence is not necessarily true for the truncated Wigner equation (see, e.g. [29]), since for example the truncation of  $\mathbf{y}$ -domain may break the Fourier completeness relation (6). Therefore, we must be more careful when doing benchmark tests for stochastic Wigner simulations by adopting the Schrödinger wavefunction as the reference, because the underlying models may not be the same. This may also explain the qualitative but not quantitative agreement shown in [22], and gives rise to the demanding for highly accurate deterministic algorithms, such as SEM [19] and the advection-spectral-mixed scheme [20], which can be used to produce a reliable reference solution as already did in [23].

### 3 The truncated Wigner equation

In order to solve numerically the Wigner equation, we need to discuss the truncated Wigner equation on a bounded domain. It should be noted that the double integrations with respect to  $\mathbf{k}'$  and  $\mathbf{y}$  in the pseudo-differential operator (see Eq. (8) or (11)) involves the infinite domain due to the Fourier transform nature, posing a formidable challenge in seeking numerical approximations. Intuitively, an feasible way is either truncating  $\mathbf{k}$ -space first or truncating  $\mathbf{y}$ -space first, denoted below by the  $k$ -truncated and  $y$ -truncated models, respectively. It is worth noting that no matter what kind of truncation we choose, the mass conservation (15) should be maintained in the resulting model as the physical requirement, which may yield additional constraints.

#### 3.1 The $k$ -truncated Wigner equation

A reasonable approach to formulate the Wigner equation in a bounded domain is to exploit the decay of the Wigner function when  $|\mathbf{k}| \rightarrow \infty$ , so that we can make the truncation in  $\mathbf{k}$ -space. Suppose that we have to evaluate the Wigner function

$f(\mathbf{x}, \mathbf{k}, t)$  in a finite domain  $\mathcal{K} = [-L_1, L_1] \times [-L_2, L_2] \cdots \times [-L_d, L_d]$  ( $L_i > 0$ ) and make a simple nullification outside  $\mathcal{K}$ , then the  $k$ -truncated Wigner equation reads

$$\frac{\partial}{\partial t} f(\mathbf{x}, \mathbf{k}, t) + \frac{\hbar \mathbf{k}}{m} \cdot \nabla_{\mathbf{x}} f(\mathbf{x}, \mathbf{k}, t) = \int_{\mathcal{K}} d\mathbf{k}' f(\mathbf{x}, \mathbf{k}', t) V_w^T(\mathbf{x}, \mathbf{k} - \mathbf{k}', t), \quad (16)$$

with the truncated Wigner kernel

$$V_w^T(\mathbf{x}, \mathbf{k}, t) = V_w(\mathbf{x}, \mathbf{k}, t) \prod_{i=1}^d \text{rect}\left(\frac{k_i}{4L_i}\right), \quad (17)$$

where the rectangular function  $\text{rect}(k)$  is given by

$$\text{rect}(k) = \begin{cases} 1, & |k| < \frac{1}{2}, \\ 0, & |k| \geq \frac{1}{2}. \end{cases} \quad (18)$$

It has to be mentioned that  $V_w^T$  is just a restriction of the Wigner kernel on a finite bandwidth  $2\mathcal{K} = [-2L_1, 2L_1] \times [-2L_2, 2L_2] \cdots \times [-2L_d, 2L_d]$ , without any change of its definition (i.e.,  $\mathbf{k} - \mathbf{k}' \in 2\mathcal{K}$  when both  $\mathbf{k}$  and  $\mathbf{k}'$  belong to  $\mathcal{K}$ ). Furthermore, it can be easily verified that

$$\int_{\mathbb{R}^d} V_w^T(\mathbf{x}, \mathbf{k}, t) d\mathbf{k} = \int_{2\mathcal{K}} V_w(\mathbf{x}, \mathbf{k}, t) d\mathbf{k} = 0, \quad (19)$$

and thus

$$\frac{d}{dt} \int_{\mathbb{R}^d} \int_{\mathcal{K}} f(\mathbf{x}, \mathbf{k}, t) d\mathbf{x} d\mathbf{k} = 0. \quad (20)$$

We expect that any reliable deterministic or stochastic method should preserve this property.

The remaining problem is to evaluate  $V_w^T$ . If the Fourier transform of  $V(\mathbf{x}, t)$  can be written in a close form  $\widehat{V}(\mathbf{k}, t)$ , we can calculate  $V_w$  directly by its definition

$$V_w(\mathbf{x}, \mathbf{k}, t) = \frac{1}{i\hbar\pi^d} (\mathbb{e}^{2i\mathbf{k}\cdot\mathbf{x}} \widehat{V}(2\mathbf{k}, t) - \mathbb{e}^{-2i\mathbf{k}\cdot\mathbf{x}} \widehat{V}(-2\mathbf{k}, t)). \quad (21)$$

Otherwise, we can still evaluate  $V_w^T$  through the Poisson summation formula

$$V_w^T(\mathbf{x}, \mathbf{k}, t) \approx \frac{1}{i\hbar(2\pi)^d} \sum_{\boldsymbol{\mu} \in \mathbb{Z}^d} \left[ \left( \prod_{i=1}^d \Delta y_i \right) D_V(\mathbf{x}, \mathbf{y}_{\boldsymbol{\mu}}, t) \mathbb{e}^{-i\mathbf{k}\cdot\mathbf{y}_{\boldsymbol{\mu}}} \right], \quad (22)$$

provided that  $V_w(\mathbf{x}, \mathbf{k})$  decays for  $|k_i| > 2|\mathcal{K}_i|$  with  $i = 1, 2, \dots, d$ . Here  $\mathbf{y}_{\boldsymbol{\mu}} = (\mu_1 \Delta y_1, \mu_2 \Delta y_2, \dots, \mu_d \Delta y_d)$  with  $y_i$  being the spacing and  $\mu_i \in \mathbb{Z}$ . In this situation, we can only follow the constraint [20]

$$2L_i \Delta y_i = 2\pi, \quad i = 1, 2, \dots, d, \quad (23)$$

to both maintain the mass conservation (20) and avoid the overlapping between  $V_w^T$  and its adjacent image.

To sum up, we would like to list several advantages of the  $k$ -truncated model.

- The  $k$ -truncated Wigner equation is defined over the continuous  $\mathbf{k}$ -space.
- It preserves the definition of the Wigner kernel and avoids the artificial periodic extension of  $D_V(\mathbf{x}, \mathbf{y}, t)$  in  $\mathbf{y}$ -space.
- When the Weyl-Wigner transform of  $V(\mathbf{x})$  has a close form, we can make use of the analytical results and avoid the artificial periodic extension of  $V_w$  in  $\mathbf{k}$ -space.

The price to pay is that the sampling in the continuous  $\mathbf{k}$ -space needs some complicated and sophisticated techniques. In general we have to resort to the Gibbs or the Metropolis sampler to tackle the high dimensional problem. We will employ in this work a simple but rather efficient rejection sampling for typical Gaussian barrier scattering tests.

### 3.2 The $y$ -truncated Wigner equation

The other way, used in [22], is based on the fact that the inverse Fourier transformed Wigner function  $\hat{f}(\mathbf{x}, \mathbf{y}, t)$  defined in Eq. (12) decays when  $|\mathbf{y}| \rightarrow \infty$ . Thus, we can focus on  $\hat{f}(\mathbf{x}, \mathbf{y}, t)$  on a bounded domain  $\mathcal{Y} = [-L_1, L_1] \times [-L_2, L_2] \cdots \times [-L_d, L_d] (L_i > 0)$ , and define the truncated pseudo-differential operator as

$$\Theta_V^T[f](\mathbf{x}, \mathbf{k}, t) = \frac{1}{i\hbar} \int_{\mathcal{Y}} d\mathbf{y} D_V(\mathbf{x}, \mathbf{y}, t) \hat{f}(\mathbf{x}, \mathbf{y}, t) e^{-i\mathbf{k} \cdot \mathbf{y}}. \quad (24)$$

In this case, we only need to evaluate  $\hat{f}(\mathbf{x}, \mathbf{y}, t)$  at a finite bandwidth through the Poisson summation formula

$$\hat{f}(\mathbf{x}, \mathbf{y}, t) \approx \frac{1}{(2\pi)^d} \sum_{\mathbf{m} \in \mathbb{Z}^d} \left[ \left( \prod_{i=1}^d \Delta k_i \right) f(\mathbf{x}, \mathbf{m}\Delta\mathbf{k}, t) e^{i\mathbf{y} \cdot \mathbf{m}\Delta\mathbf{k}} \right], \quad \mathbf{y} \in \mathcal{Y}. \quad (25)$$

under the assumption that it decays when  $y_i > L_i$ . Here  $\mathbf{m}\Delta\mathbf{k} = (m_1\Delta k_1, m_2\Delta k_2, \dots, m_d\Delta k_d)$  with  $\Delta k_i$  being the spacing,  $m_i \in \mathbb{Z}$ ,  $i = 1, 2, \dots, d$ . Substituting Eq. (25) into Eq. (24) leads to

$$\Theta_V^T[f](\mathbf{x}, \mathbf{k}, t) \approx \sum_{\mathbf{m} \in \mathbb{Z}^d} f(\mathbf{x}, \mathbf{m}\Delta\mathbf{k}, t) \tilde{V}_w(\mathbf{x}, \mathbf{k} - \mathbf{m}\Delta\mathbf{k}, t), \quad (26)$$

$$\tilde{V}_w(\mathbf{x}, \mathbf{k}, t) = \frac{1}{i\hbar} \frac{1}{|\mathcal{Y}|} \int_{\mathcal{Y}} d\mathbf{y} D_V(\mathbf{x}, \mathbf{y}, t) e^{-i\mathbf{y} \cdot \mathbf{k}}. \quad (27)$$

Here we have let  $|\mathcal{Y}| = 2L_1 \times 2L_2 \cdots \times 2L_d$  and used the constraint

$$2L_i \Delta k_i = 2\pi, \quad i = 1, 2, \dots, d, \quad (28)$$

which serves as the sufficient and necessary condition to establish the semi-discrete mass conversation

$$\frac{d}{dt} \int_{\mathbb{R}^d} d\mathbf{x} \sum_{\mathbf{n} \in \mathbb{Z}^d} f(\mathbf{x}, \mathbf{n}\Delta\mathbf{k}, t) \Delta\mathbf{k} = 0. \quad (29)$$



Suppose the Wigner function at discrete samples  $\mathbf{k} = \mathbf{n}\Delta\mathbf{k}$  are wanted, then we immediately arrive at the  $y$ -truncated (or semi-discrete) Wigner equation

$$\begin{aligned} \frac{\partial}{\partial t} f(\mathbf{x}, \mathbf{n}\Delta\mathbf{k}, t) + \frac{\hbar \mathbf{n}\Delta\mathbf{k}}{m} \cdot \nabla_{\mathbf{x}} f(\mathbf{x}, \mathbf{n}\Delta\mathbf{k}, t) \\ = \sum_{\mathbf{m} \in \mathbb{Z}^d} f(\mathbf{x}, \mathbf{m}\Delta\mathbf{k}, t) \tilde{V}_w(\mathbf{x}, \mathbf{n}\Delta\mathbf{k} - \mathbf{m}\Delta\mathbf{k}, t), \end{aligned} \quad (30)$$

which indeed provides a straightforward way for stochastic simulations as used in the spWMC method, and possesses the following properties.

- The modified Wigner kernel  $\tilde{V}_w$  in Eq. (27) can be treated as the Fourier coefficients of  $D_V(\mathbf{x}, \mathbf{y}, t)$  (with a periodic extension), and can be recovered by the inverse Fourier transform (possibly by the inverse fast Fourier transform).
- The continuous convolution is now replaced by a discrete convolution (see Eqs. (8) and (26)), so that the sampling in discrete  $\mathbf{k}$ -space can be simply realized by counting the cumulative distribution function.
- The set of equidistant sampling in  $\mathbf{k}$ -space facilitates the data storage.

However, the major disadvantage of the  $y$ -truncated model is, the modified Wigner potential  $\tilde{V}_w$  is not a trivial approximation to the original Wigner potential (one can refer to the difference between the Fourier coefficients and continuous Fourier transformation). The convergence  $\tilde{V}_w \rightarrow V_w$  is only valid when  $|\mathcal{Y}| \rightarrow \infty$ , or the potential  $V(\mathbf{x}, t)$  decays rapidly at the boundary of the finite domain (but this condition is not true for, e.g., the Coulomb-like potential, especially for the Coulomb interaction between two particles). By contrast, the  $k$ -truncated model only requires the decay of the Wigner function in  $\mathbf{k}$ -space, and can make full use of several analytical results of the Wigner kernel. Personally speaking, we would like to stress that *the  $k$ -truncated Wigner equation is more appropriate for simulating many-body quantum systems.*

## 4 Renewal-type integral equations

In order to build the connection between the deterministic partial integro-differential equation (7) and a stochastic process, we first cast the deterministic equation into a renewal-type integral equation. For this purpose, the first crucial step is to introduce an exponential distribution in its integral formulation via *an auxiliary function*  $\gamma(x)$ . The second one is to split the Wigner kernel into two positive parts [27], such that each part can be endowed with a probabilistic interpretation. More importantly, to make the resulting stochastic Wigner branching process computable, an equivalent representation of the inner product (3) is derived by exploiting the adjoint equation.

Without loss of generality, in the subsequent discussion we focus on the  $k$ -truncated Wigner equation (16), and a similar idea can be straightforwardly generalized to the  $y$ -truncated equation (30) as well as the original Wigner equation (7).

## 4.1 Integral formulation with an auxiliary function

The first step is to cast Eq. (16) into a renewal-type equation. To this end, we can introduce an auxiliary function  $\gamma(\mathbf{x})$  and add the term  $\gamma(\mathbf{x})f(\mathbf{x}, \mathbf{k}, t)$  in both sides of Eq. (16), yielding

$$\begin{aligned} \frac{\partial}{\partial t} f(\mathbf{x}, \mathbf{k}, t) + \frac{\hbar \mathbf{k}}{m} \cdot \nabla_{\mathbf{x}} f(\mathbf{x}, \mathbf{k}, t) + \gamma(\mathbf{x}) f(\mathbf{x}, \mathbf{k}, t) \\ = \int_{\mathcal{K}} d\mathbf{k}' f(\mathbf{x}, \mathbf{k}', t) [V_w(\mathbf{x}, \mathbf{k} - \mathbf{k}', t) + \gamma(\mathbf{x}) \delta(\mathbf{k} - \mathbf{k}')]. \end{aligned} \quad (31)$$

At this stage, we only consider a nonnegative bounded  $\gamma(\mathbf{x})$ , though a time-dependent  $\gamma(\mathbf{x}, t)$  can be also introduced if necessary and analyzed in a similar way. In particular, *we strongly recommend to choose a constant*  $\gamma(\mathbf{x}) \equiv \gamma_0$  in real applications, for the convenience of both theoretical analysis and numerical computation (vide post). Formally, we can write down its integral formulation through the variation-of-constant formula

$$f(\mathbf{x}, \mathbf{k}, t) = e^{t\mathcal{A}} f(\mathbf{x}, \mathbf{k}, 0) + \int_0^t e^{(t-t')\mathcal{A}} [\mathcal{B}(\mathbf{x}, \mathbf{k}, t') + \gamma(\mathbf{x})] f(\mathbf{x}, \mathbf{k}, t') dt', \quad (32)$$

where  $e^{t\mathcal{A}}$  denotes the semigroup generated by the operator

$$\mathcal{A} = -\hbar \mathbf{k} / m \cdot \nabla_{\mathbf{x}} - \gamma(\mathbf{x}), \quad (33)$$

and

$$\mathcal{B}(\mathbf{x}, \mathbf{k}, t) f(\mathbf{x}, \mathbf{k}, t) = \int_{\mathcal{K}} d\mathbf{k}' f(\mathbf{x}, \mathbf{k}', t) V_w(\mathbf{x}, \mathbf{k} - \mathbf{k}', t) \quad (34)$$

is the convolution operator which is assumed to be a bounded operator throughout this work.

When  $\gamma(\mathbf{x})$  is bounded, it only imposes a Lyapunov perturbation on a hyperbolic system, so that the operator  $e^{t\mathcal{A}}$  is also a  $C_0$ -semigroup [30]. To further determine how the operator  $e^{t\mathcal{A}}$  acts on a given function  $u(\mathbf{x}, \mathbf{k}, t) \in C^1(L^2(\mathbb{R}^{2d}), [0, T])$ , we need to solve the following evolution system

$$\frac{\partial}{\partial t} u(\mathbf{x}, \mathbf{k}, t) + \frac{\hbar \mathbf{k}}{m} \cdot \nabla_{\mathbf{x}} u(\mathbf{x}, \mathbf{k}, t) + \gamma(\mathbf{x}) u(\mathbf{x}, \mathbf{k}, t) = 0. \quad (35)$$

After performing the coordinate conversion [31]

$$\begin{cases} \mathbf{x}' = \mathbf{x} - \hbar \mathbf{k} t / m, \\ \mathbf{k}' = \mathbf{k}, \\ t' = t, \end{cases} \quad (36)$$

we obtain

$$\frac{\partial}{\partial t'} u'(\mathbf{x}', \mathbf{k}', t') = -\gamma'(\mathbf{x}', t') u'(\mathbf{x}', \mathbf{k}', t'), \quad (37)$$

where  $u'(\mathbf{x}', \mathbf{k}', t') := u(\mathbf{x}, \mathbf{k}, t)$  and  $\gamma'(\mathbf{x}', t') := \gamma(\mathbf{x}' + \hbar \mathbf{k}' t' / m) = \gamma(\mathbf{x})$ . The solution to the above system reads

$$u'(\mathbf{x}', \mathbf{k}', t') = e^{-\int_0^{t'} \gamma'(\mathbf{x}', s) ds} u'(\mathbf{x}', \mathbf{k}', 0). \quad (38)$$

Replacing  $u', \gamma'$  by  $u, \gamma$  and making a shift  $\mathbf{x}' \rightarrow \mathbf{x} = \mathbf{x}' + \hbar \mathbf{k} t / m$  in Eq. (38) leads to

$$e^{tA} u(\mathbf{x}, \mathbf{k}, 0) = e^{-\int_0^t \gamma(\mathbf{x}(t-s)) ds} u(\mathbf{x}(t), \mathbf{k}, 0), \quad (39)$$

where

$$\mathbf{x}(\Delta t) = \mathbf{x} - \hbar \mathbf{k} \Delta t / m \quad (40)$$

is termed the *backward-in-time trajectory* of  $(\mathbf{x}, \mathbf{k})$  with a positive time increment  $\Delta t$ .

After a simple variable substitution ( $s + t' \rightarrow s$ ), the integral formulation of the Wigner equation becomes

$$\begin{aligned} f(\mathbf{x}, \mathbf{k}, t) = & e^{-\int_0^t \gamma(\mathbf{x}(t-s)) ds} f(\mathbf{x}(t), \mathbf{k}, 0) + \int_0^t dt' e^{-\int_{t'}^t \gamma(\mathbf{x}(t-s)) ds} \\ & \times [\mathcal{B}(\mathbf{x}(t-t'), \mathbf{k}, t') + \gamma(\mathbf{x}(t-t'))] f(\mathbf{x}(t-t'), \mathbf{k}, t'). \end{aligned} \quad (41)$$

Let

$$\mathcal{H}(t'; \mathbf{x}, t) = 1 - \int_{t'}^t \gamma(\mathbf{x}(t-\tau)) e^{-\int_\tau^t \gamma(\mathbf{x}(t-s)) ds} d\tau, \quad (42)$$

and assume the auxiliary function satisfies

$$\gamma(\mathbf{x}) \geq 0, \quad \lim_{t' \rightarrow -\infty} \int_{t'}^t \gamma(\mathbf{x}(t-s)) ds = +\infty, \quad \forall \mathbf{x} \in \mathbb{R}^d, \quad (43)$$

then we have

$$d\mathcal{H}(t'; \mathbf{x}, t) \geq 0, \quad \int_{-\infty}^t d\mathcal{H}(t'; \mathbf{x}, t) = 1, \quad (44)$$

implying that  $\mathcal{H}(t'; \mathbf{x}, t)$  is a probability measure with respect to  $t'$  for a given  $(\mathbf{x}, t)$  on  $t' \leq t$ , characterized by the auxiliary function  $\gamma(\mathbf{x})$ . Substituting this measure into Eq. (41) gives

$$\begin{aligned} f(\mathbf{x}, \mathbf{k}, t) = & [1 - \mathcal{H}(0; \mathbf{x}, t)] f(\mathbf{x}(t), \mathbf{k}, 0) + \int_0^t d\mathcal{H}(t'; \mathbf{x}, t) \times \\ & \int_{\mathcal{K}} d\mathbf{k}' f(\mathbf{x}(t-t'), \mathbf{k}', t') \left\{ \frac{V_w(\mathbf{x}(t-t'), \mathbf{k} - \mathbf{k}', t')}{\gamma(\mathbf{x}(t-t'))} + \delta(\mathbf{k} - \mathbf{k}') \right\}, \end{aligned} \quad (45)$$

which can be regarded as a *kind of renewal-type equation* in the renewal theory [32, 33].

Next we turn to consider the Wigner kernel  $V_w$ , that cannot be regarded as a transition kernel directly as it allows negative values. Nevertheless, we can split it into two positive semidefinite parts as follows

$$V_w(\mathbf{x}, \mathbf{k}, t) = V_w^+(\mathbf{x}, \mathbf{k}, t) - V_w^-(\mathbf{x}, \mathbf{k}, t) \quad (46)$$

where

$$V_w^+(\mathbf{x}, \mathbf{k}, t) = \frac{1}{2} |V_w(\mathbf{x}, \mathbf{k}, t)| + \frac{1}{2} V_w(\mathbf{x}, \mathbf{k}, t), \quad (47)$$

$$V_w^-(\mathbf{x}, \mathbf{k}, t) = \frac{1}{2} |V_w(\mathbf{x}, \mathbf{k}, t)| - \frac{1}{2} V_w(\mathbf{x}, \mathbf{k}, t). \quad (48)$$

Owing to the anti-symmetry of  $V_w$  (see Eq. (13)), it can be easily verified that

$$V_w^+(\mathbf{x}, \mathbf{k}, t) = V_w^-(\mathbf{x}, -\mathbf{k}, t). \quad (49)$$

We further define a function  $\Gamma$  on  $t \geq t'$ , composed of three terms

$$\begin{aligned} \Gamma(\mathbf{x}(t-t'), \mathbf{k}, t; \mathbf{x}', \mathbf{k}', t') = & V_w^+(\mathbf{x}(t-t'), \mathbf{k} - \mathbf{k}', t') \cdot \delta(\mathbf{x}(t-t') - \mathbf{x}') \\ & - V_w^-(\mathbf{x}(t-t'), \mathbf{k} - \mathbf{k}', t') \cdot \delta(\mathbf{x}(t-t') - \mathbf{x}') \\ & + \gamma(\mathbf{x}(t-t')) \cdot \delta(\mathbf{k} - \mathbf{k}') \cdot \delta(\mathbf{x}(t-t') - \mathbf{x}'). \end{aligned} \quad (50)$$

Finally, the  $k$ -truncated Wigner equation (16) can be cast into a Fredholm integral equation of the second kind

$$f(\mathbf{x}, \mathbf{k}, t) = f_0(\mathbf{x}, \mathbf{k}, t) + \mathcal{S}f(\mathbf{x}, \mathbf{k}, t), \quad 0 \leq t \leq T, \quad (51)$$

where

$$f_0(\mathbf{x}, \mathbf{k}, t) = \mathbb{E}^{-\int_0^t \gamma(\mathbf{x}(t-s)) ds} f(\mathbf{x}(t), \mathbf{k}, 0), \quad (52)$$

$$\mathcal{S}f(\mathbf{x}, \mathbf{k}, t) = \int_0^t dt' \int_{\mathbb{R}^d} d\mathbf{x}' \int_{\mathcal{K}} d\mathbf{k}' K(\mathbf{x}, \mathbf{k}, t; \mathbf{x}', \mathbf{k}', t') f(\mathbf{x}', \mathbf{k}', t'), \quad (53)$$

$$K(\mathbf{x}, \mathbf{k}, t; \mathbf{x}', \mathbf{k}', t') = \mathbb{E}^{-\int_{t'}^t \gamma(\mathbf{x}(t-s)) ds} \Gamma(\mathbf{x}(t-t'), \mathbf{k}, t; \mathbf{x}', \mathbf{k}', t'), \quad t \geq t'. \quad (54)$$

Before discussing the probabilistic approach to the integral equation (51), we would like first to derive its adjoint equation and attain an equivalent representation of  $\langle A \rangle_T$ , which serves as the cornerstone of the computable Wigner branching process in numerics.

## 4.2 Dual system and adjoint equation

In quantum mechanics, we are often interested in macroscopically measurable quantities  $\langle A \rangle_t$ , such as the Wigner probability, electron density, etc. In this regard, we turn to consider the problem of evaluating the inner product

$$\langle g_0, f \rangle = \int_0^T dt \int_{\mathbb{R}^d} d\mathbf{x} \int_{\mathcal{K}} d\mathbf{k} g_0(\mathbf{x}, \mathbf{k}, t) f(\mathbf{x}, \mathbf{k}, t), \quad (55)$$

on the domain  $\mathbb{R}^d \times \mathcal{K} \times [0, T]$  ( $T > 0$ ). For instance, to evaluate the average value  $\langle A \rangle_T$  of a macroscopic quantity  $A(\mathbf{x}, \mathbf{k})$  at a given final time  $T$ , we should take

$$g_0(\mathbf{x}, \mathbf{k}, t) = A(\mathbf{x}, \mathbf{k}) \delta(t - T), \quad (56)$$

then

$$\langle A \rangle_T = \langle g_0, f \rangle. \quad (57)$$

In this section, we will give the explicit formulation of the adjoint equation, starting from Eq. (51) and Eq. (56). For brevity, we will assume that the potential is time-independent, and thus the kernels becomes

$$K(\mathbf{x}, \mathbf{k}, t; \mathbf{x}', \mathbf{k}', t') = \mathbb{E}^{-\int_{t'}^t \gamma(\mathbf{x}(t-s)) ds} \Gamma(\mathbf{x}(t-t'), \mathbf{k}; \mathbf{x}', \mathbf{k}'), \quad t \geq t', \quad (58)$$

$$\Gamma(\mathbf{x}, \mathbf{k}; \mathbf{x}', \mathbf{k}') = [V_w^+(\mathbf{x}, \mathbf{k} - \mathbf{k}') - V_w^-(\mathbf{x}, \mathbf{k} - \mathbf{k}') + \gamma(\mathbf{x})\delta(\mathbf{k} - \mathbf{k}')] \delta(\mathbf{x} - \mathbf{x}'). \quad (59)$$

Suppose the kernel  $K(\mathbf{x}, \mathbf{k}, t; \mathbf{x}', \mathbf{k}', t')$  is bounded, then it's easy to verify that  $\mathcal{S}$  is a bounded linear operator. Accordingly, we can define the adjoint operator  $\mathcal{T} = \mathcal{S}^*$  by

$$\langle g, \mathcal{S}f \rangle = \langle \mathcal{S}^*g, f \rangle = \langle \mathcal{T}g, f \rangle, \quad (60)$$

Applying Theorem 4.6 in [34] directly into the Fredholm integral equation of the second kind (51) yields

$$\mathcal{T}g(\mathbf{x}', \mathbf{k}', t') = \int_{t'}^T dt \int_{\mathbb{R}^d} d\mathbf{x} \int_{\mathcal{K}} d\mathbf{k} K(\mathbf{x}, \mathbf{k}, t; \mathbf{x}', \mathbf{k}', t') g(\mathbf{x}, \mathbf{k}, t), \quad t \geq t'. \quad (61)$$

Formally, it suffices to define

$$g(\mathbf{x}', \mathbf{k}', t') = \mathcal{T}g(\mathbf{x}', \mathbf{k}', t') + g_0(\mathbf{x}', \mathbf{k}', t'), \quad 0 \leq t' \leq T. \quad (62)$$

Since

$$\langle g, f \rangle = \langle g, \mathcal{S}f + f_0 \rangle = \langle \mathcal{T}g, f \rangle + \langle g, f_0 \rangle = \langle g, f \rangle - \langle g_0, f \rangle + \langle g, f_0 \rangle, \quad (63)$$

we have

$$\langle g_0, f \rangle = \langle g, f_0 \rangle, \quad (64)$$

namely

$$\langle A \rangle_T = \int_0^T dt' \int_{\mathbb{R}^d} d\mathbf{x}' \int_{\mathcal{K}} d\mathbf{k}' f(\mathbf{x}'(t'), \mathbf{k}', 0) \mathbb{E}^{-\int_0^{t'} \gamma(\mathbf{x}'(t'-s)) ds} g(\mathbf{x}', \mathbf{k}', t'). \quad (65)$$

Furthermore, we perform the coordinate conversion

$$\begin{cases} \mathbf{r}_0 = \mathbf{x}'(t') = \mathbf{x}' - \hbar \mathbf{k}' t' / m, \\ \mathbf{k}_0 = \mathbf{k}', \\ t_0 = t', \end{cases} \quad (66)$$

with which the Jacobian determinant  $\frac{\partial(\mathbf{r}_0, \mathbf{k}_0, t_0)}{\partial(\mathbf{x}', \mathbf{k}', t')} = 1$  implying the volume unit keeps unchanged (i.e.,  $d\mathbf{r}_0 d\mathbf{k}_0 dt = d\mathbf{x}' d\mathbf{k}' dt'$ ), and thus Eq. (65) becomes

$$\langle A \rangle_T = \int_0^T dt_0 \int_{\mathbb{R}^d} d\mathbf{r}_0 \int_{\mathcal{K}} d\mathbf{k}_0 f(\mathbf{r}_0, \mathbf{k}_0, 0) \mathbb{E}^{-\int_0^{t_0} \gamma(\mathbf{r}_0(s)) ds} g(\mathbf{r}_0(t_0), \mathbf{k}_0, t_0), \quad (67)$$

where we have introduced a *forward-in-time trajectory* (in contrast to the backward-in-time trajectory  $\mathbf{x}(\Delta t)$  given in Eq. (40)) as follows

$$\mathbf{r}_0(\Delta t) = \mathbf{r}_0 + \hbar \mathbf{k}_0 \Delta t / m, \quad (68)$$

with  $\Delta t \geq 0$  being the time increment. Actually, Eq. (67) motivates us to combine the exponential factor with  $g$  and define a new function  $\varphi(\mathbf{r}, \mathbf{k}, t) \in C^1(L^2(\mathbb{R}^d \times \mathcal{K}), [0, T])$  as

$$\varphi(\mathbf{r}, \mathbf{k}, t) = \int_t^T dt' e^{-\int_t^{t'} \gamma(\mathbf{r}(s-t)) ds} g(\mathbf{r}(t' - t), \mathbf{k}, t'). \quad (69)$$

Please keep in mind that, it is required  $t' \geq t$  for convenience in the definition (69), before which  $t' \leq t$  is always assumed, for example, see Eq. (61). Consequently, from Eq. (67), the inner product (57) can be determined *only by the ‘initial’ data*, as stated in the following theorem.

**Theorem 1.** *The average value  $\langle A \rangle_T$  of a macroscopic quantity  $A(\mathbf{x}, \mathbf{k})$  at a given final time  $T$  can be evaluated by*

$$\langle A \rangle_T = \int_{\mathbb{R}^d} d\mathbf{r}_0 \int_{\mathcal{K}} d\mathbf{k}_0 f(\mathbf{r}_0, \mathbf{k}_0, 0) \varphi(\mathbf{r}_0, \mathbf{k}_0, 0), \quad (70)$$

where  $\varphi$  is defined in Eq. (69).

According to Eq. (70), in order to evaluate  $\langle A \rangle_T$ , the remaining task is to calculate  $\varphi(\mathbf{r}_0, \mathbf{k}_0, 0)$ . To this end, we need first to obtain the expression of  $g(\mathbf{r}_0(t_0), \mathbf{k}_0, t_0)$  from the dual system (62).

Replacing  $(\mathbf{x}', \mathbf{k}', t')$  by  $(\mathbf{r}_0(t_0), \mathbf{k}_0, t_0)$  and performing the coordinate conversion  $\mathbf{x}(t - t') \rightarrow \mathbf{r}_1, \mathbf{k} \rightarrow \mathbf{k}_1, t \rightarrow t_1$  in Eq. (62) yield

$$\begin{aligned} g(\mathbf{r}_0(t_0), \mathbf{k}_0, t_0) = & g_0(\mathbf{r}_0(t_0), \mathbf{k}_0, t_0) + \int_{t_0}^T dt_1 \int_{\mathbb{R}^d} d\mathbf{r}_1 \int_{\mathcal{K}} d\mathbf{k}_1 e^{-\int_{t_0}^{t_1} \gamma(\mathbf{r}_1(s-t_0)) ds} \\ & \times \Gamma(\mathbf{r}_1, \mathbf{k}_1; \mathbf{r}_0(t_0), \mathbf{k}_0) g(\mathbf{r}_1(t_1 - t_0), \mathbf{k}_1, t_1), \end{aligned} \quad (71)$$

where the trajectory  $\mathbf{r}_1(\Delta t)$  reads

$$\mathbf{r}_1(\Delta t) = \mathbf{r}_1 + \hbar \mathbf{k}_1 \Delta t / m, \quad \Delta t \geq 0, \quad (72)$$

which is *not* the same as  $\mathbf{r}_0(\Delta t)$  given in Eq. (68) since the underlying wavevectors  $\mathbf{k}_0$  and  $\mathbf{k}_1$  are different! Substituting Eq. (71) into Eq. (67) leads to

$$\begin{aligned} \langle A \rangle_T = & \langle A \rangle_{T,0} + \int_0^T dt_0 \int_{\mathbb{R}^d} d\mathbf{r}_0 \int_{\mathcal{K}} d\mathbf{k}_0 f(\mathbf{r}_0, \mathbf{k}_0, 0) e^{-\int_0^{t_0} \gamma(\mathbf{r}_0(s)) ds} \int_{t_0}^T dt_1 \\ & \times \int_{\mathbb{R}^d} d\mathbf{r}_1 \int_{\mathcal{K}} d\mathbf{k}_1 e^{-\int_{t_0}^{t_1} \gamma(\mathbf{r}_1(s-t_0)) ds} \Gamma(\mathbf{r}_1, \mathbf{k}_1; \mathbf{r}_0(t_0), \mathbf{k}_0) g(\mathbf{r}_1(t_1 - t_0), \mathbf{k}_1, t_1), \end{aligned} \quad (73)$$

where

$$\langle A \rangle_{T,0} = \int_{\mathbb{R}^d} d\mathbf{r}_0 \int_{\mathcal{K}} d\mathbf{k}_0 f(\mathbf{r}_0, \mathbf{k}_0, 0) e^{-\int_0^T \gamma(\mathbf{r}_0(s)) ds} A(\mathbf{r}_0(T), \mathbf{k}_0). \quad (74)$$

From the dual system (62), we can also obtain a similar expression to Eq. (71) for  $g(\mathbf{r}_1(t_1 - t_0), \mathbf{k}_1, t_1)$ , and then corresponding time integration with respect to  $t_1$  in Eq. (73) becomes

$$\begin{aligned} & \int_{t_0}^T dt_1 e^{-\int_{t_0}^{t_1} \gamma(\mathbf{r}_1(s-t_0))ds} g(\mathbf{r}_1(t_1 - t_0), \mathbf{k}_1, t_1) = e^{-\int_{t_0}^T \gamma(\mathbf{r}_1(s-t_0))ds} A(\mathbf{r}_1(T - t_0), \mathbf{k}_1) \\ & + \int_{t_0}^T dt_1 e^{-\int_{t_0}^{t_1} \gamma(\mathbf{r}_1(s-t_0))ds} \int_{t_1}^T dt_2 \int_{\mathbb{R}^d} d\mathbf{r}_2 \int_{\mathcal{K}} d\mathbf{k}_2 g(\mathbf{r}_2(t_2 - t_1), \mathbf{k}_2, t_2) \\ & \times e^{-\int_{t_1}^{t_2} \gamma(\mathbf{r}_2(s-t_1))ds} \Gamma(\mathbf{r}_2, \mathbf{k}_2; \mathbf{r}_1(t_1 - t_0), \mathbf{k}_1), \end{aligned} \quad (75)$$

where

$$\mathbf{r}_2(\Delta t) = \mathbf{r}_2 + \hbar \mathbf{k}_2 \Delta t / m, \quad \Delta t \geq 0. \quad (76)$$

Combining Eq. (75) and the definition (69) directly gives the adjoint equation for  $\varphi$  as stated in Theorem 2.

**Theorem 2** (Adjoint equation). *The function  $\varphi(\mathbf{r}, \mathbf{k}, t)$  defined in Eq. (69) satisfies the following integral equation*

$$\begin{aligned} \varphi(\mathbf{r}, \mathbf{k}, t) = & e^{-\int_t^T \gamma(\mathbf{r}(s-t))ds} A(\mathbf{r}(T - t), \mathbf{k}) + \int_t^T dt' \int_{\mathbb{R}^d} d\mathbf{r}' \int_{\mathcal{K}} d\mathbf{k}' \\ & \times \varphi(\mathbf{r}', \mathbf{k}', t') e^{-\int_t^{t'} \gamma(\mathbf{r}(s-t))ds} \Gamma(\mathbf{r}', \mathbf{k}'; \mathbf{r}(t' - t), \mathbf{k}). \end{aligned} \quad (77)$$

We call Eq. (77) the adjoint equation of Eq. (41) is mainly because  $f(\mathbf{r}, \mathbf{k}, 0)$  and  $\varphi(\mathbf{r}, \mathbf{k}, 0)$  constitute a dual system in the bilinear form (70) (denoted by  $\langle \cdot, \cdot \rangle_0$ ) for determining  $\langle A \rangle_T$ . Combining the formal solution  $f(\mathbf{r}, \mathbf{k}, T) = e^{T(\mathcal{A}+\mathcal{B})} f(\mathbf{r}, \mathbf{k}, 0)$  of the Wigner equation (16) as well as Eqs. (3) and (70) directly yields

$$\begin{aligned} \langle A \rangle_T = & \langle f(\mathbf{r}, \mathbf{k}, 0), \varphi(\mathbf{r}, \mathbf{k}, 0) \rangle_0 = \langle f(\mathbf{r}, \mathbf{k}, T), A(\mathbf{r}, \mathbf{k}) \rangle_0 \\ = & \langle e^{T(\mathcal{A}+\mathcal{B})} f(\mathbf{r}, \mathbf{k}, 0), A(\mathbf{r}, \mathbf{k}) \rangle_0 = \langle f(\mathbf{r}, \mathbf{k}, 0), e^{-T(\mathcal{A}+\mathcal{B})} A(\mathbf{r}, \mathbf{k}) \rangle_0. \end{aligned} \quad (78)$$

In consequence, we formally obtain  $\varphi(\mathbf{r}, \mathbf{k}, 0) = e^{-T(\mathcal{A}+\mathcal{B})} A(\mathbf{r}, \mathbf{k})$  with  $e^{-T(\mathcal{A}+\mathcal{B})}$  being the adjoint operator of  $e^{T(\mathcal{A}+\mathcal{B})}$ , indicating that Eq. (77), in some sense, can be treated as an inverse problem of Eq. (51), which produces a quantity  $\varphi(\mathbf{r}, \mathbf{k}, 0)$  from the observation  $A(\mathbf{r}, \mathbf{k})$  at the ending time  $T$ .

Moreover, for given  $(\mathbf{r}, t)$  on  $t' \geq t$ , we can similarly introduce a probability measure with respect to  $t'$  like

$$\mathcal{G}(t'; \mathbf{r}, t) = \int_t^{t'} \gamma(\mathbf{r}(\tau - t)) e^{-\int_t^\tau \gamma(\mathbf{r}(s-t))ds} d\tau, \quad (79)$$

because of

$$d\mathcal{G}(t'; \mathbf{r}, t) \geq 0, \quad \int_t^{+\infty} d\mathcal{G}(t'; \mathbf{r}, t) = 1, \quad (80)$$

under the assumption that the auxiliary function satisfies

$$\forall \mathbf{r} \in \mathbb{R}^d, \quad \gamma(\mathbf{r}) \geq 0, \quad \lim_{t' \rightarrow +\infty} \int_t^{t'} \gamma(\mathbf{r}(t - s))ds = +\infty. \quad (81)$$

Substituting the measure (79) into Eq. (77) also yields a renewal-type equation

$$\begin{aligned} \varphi(\mathbf{r}, \mathbf{k}, t) = & [1 - \mathcal{G}(T; \mathbf{r}, t)] A(\mathbf{r}(T - t), \mathbf{k}) \\ & + \int_t^T d\mathcal{G}(t'; \mathbf{r}, t) \int_{\mathbb{R}^d} d\mathbf{r}' \int_{\mathcal{K}} d\mathbf{k}' \frac{\Gamma(\mathbf{r}', \mathbf{k}'; \mathbf{r}(t' - t), \mathbf{k})}{\gamma(\mathbf{r}(t' - t))} \varphi(\mathbf{r}', \mathbf{k}', t'). \end{aligned} \quad (82)$$

## 5 The Wigner branching process

Owing to the fact that all the moments of a branching process satisfy the renewal-type equations [32], it naturally motivates us to construct a branching process such that its expectation is the unique solution of Eq. (45) or Eq. (82). Hereafter we will denote such a random process by the *Wigner branching process* and introduce a probabilistic model, termed the branching particle system, to describe it in a picturesque language. In numerics, the solution at  $(\mathbf{r}, \mathbf{k}, t)$  can be obtained by tracking the branching history of weighted super-particles. The particle trajectories are either backward or forward in time, depending on the temporal flow direction. We will devote to validating such a probabilistic approach, studying the inherent mass conservation property and deriving a basic estimate on the growth of particle number.

Before getting into the details of stochastic Wigner solvers, we would like to emphasize the central role of Eq. (70) in the computable Wigner branching process. In fact, combining the probabilistic approach with the principle of importance sampling, the inner product (57) can be evaluated by a purely particle-based scheme in which every super-particle, carrying a weight and a sign, is moving according to several specific rules in the branching particle system. More importantly, such stochastic method allows us to solve the Wigner quantum dynamics in a time-marching manner and annihilate the super-particles with opposite signs, thereby overcoming the potential weakness of the branching process treatment, such as the exponential growth of particle number, and successfully saving the efficiency.

### 5.1 Importance sampling

Hereto we have shown in Eq. (70) that the average  $\langle A \rangle_T$  can be evaluated by sampling from the initial Wigner function  $f(\mathbf{r}, \mathbf{k}, 0)$  and solving the adjoint equation (77) for  $\varphi(\mathbf{r}, \mathbf{k}, 0)$ , instead of the direct calculation based on  $f(\mathbf{r}, \mathbf{k}, T)$  as shown in Eq. (57). Actually, the bilinear form (70) for determining  $\langle A \rangle_T$  serves as the foundation of the so-called Wigner Monte Carlo algorithm in which the importance sampling plays a key role.

In order to calculate  $\langle A \rangle_t$ , two major obstacles must be overcome, one is how to seek a numerical approximation to the Wigner function, the other is how to draw samples according to it. To this end, a simple function  $f_S$  is introduced first as follows

$$f_S(\mathbf{x}, \mathbf{k}, t) = \sum_j 1_{D_j}(\mathbf{x}, \mathbf{k}) \cdot \frac{1}{|D_j|} \cdot \iint_{D_j} f(\mathbf{x}, \mathbf{k}, t) d\mathbf{x} d\mathbf{k}, \quad (83)$$



where  $\{D_j\}$  gives a partition of  $\mathbb{R}^d \times \mathcal{K}$ . It can be easily found that  $f_S(\mathbf{x}, \mathbf{k}, t)$  converges to  $f(\mathbf{x}, \mathbf{k}, t)$  as  $|D_j| \rightarrow 0$ , and satisfies

$$\iint_{\mathbb{R}^d \times \mathcal{K}} f_S(\mathbf{x}, \mathbf{k}, t) d\mathbf{x} d\mathbf{k} = \iint_{\mathbb{R}^d \times \mathcal{K}} f(\mathbf{x}, \mathbf{k}, t) d\mathbf{x} d\mathbf{k} = 1. \quad (84)$$

Hereafter the simple function  $f_S$  serves as the numerical approximation to the Wigner function  $f$ .

Regarding of the fact that the Wigner function may take negative value, we further introduce an *instrumental probability distribution*  $f_I$  as follows

$$f_I(\mathbf{x}, \mathbf{k}, t) = \frac{1}{H(t)} \sum_j 1_{D_j}(\mathbf{x}, \mathbf{k}) \cdot \frac{1}{|D_j|} \cdot \left| \iint_{D_j} f(\mathbf{x}, \mathbf{k}, t) d\mathbf{x} d\mathbf{k} \right|, \quad (85)$$

where  $H(t)$  is the normalization factor (we assume  $H(t)$  is bounded)

$$H(t) = \sum_j \left| \iint_{D_j} f(\mathbf{x}, \mathbf{k}, t) d\mathbf{x} d\mathbf{k} \right|. \quad (86)$$

It can be easily verified that

$$f_I(\mathbf{x}, \mathbf{k}, t) H(t) = |f_S(\mathbf{x}, \mathbf{k}, t)|. \quad (87)$$

Sampling from the distribution (85) is quite convenient since it is equivalent to allocating super-particles in each cell  $D_j$ , according to the absolute value of the Wigner quasi-probability  $\iint_{D_j} f(\mathbf{x}, \mathbf{k}, t) d\mathbf{x} d\mathbf{k}$  and the volume  $|D_j|$ . In consequence, we can simply approximate  $\langle A \rangle_t$  from Eq. (57) by

$$\begin{aligned} \langle A \rangle_t &= \iint_{\mathbb{R}^d \times \mathcal{K}} A(\mathbf{x}, \mathbf{k}) \cdot \frac{f(\mathbf{x}, \mathbf{k}, t)}{f_S(\mathbf{x}, \mathbf{k}, t)} \cdot \frac{f_S(\mathbf{x}, \mathbf{k}, t)}{f_I(\mathbf{x}, \mathbf{k}, t)} \cdot f_I(\mathbf{x}, \mathbf{k}, t) d\mathbf{x} d\mathbf{k} \\ &\approx \iint_{\mathbb{R}^d \times \mathcal{K}} A(\mathbf{x}, \mathbf{k}) \cdot \frac{f_S(\mathbf{x}, \mathbf{k}, t)}{f_I(\mathbf{x}, \mathbf{k}, t)} \cdot f_I(\mathbf{x}, \mathbf{k}, t) d\mathbf{x} d\mathbf{k} \approx \sum_{\alpha} A(\mathbf{x}_{\alpha}, \mathbf{k}_{\alpha}) \cdot w_{\alpha}(t), \end{aligned} \quad (88)$$

where the first approximation utilizes the fact that  $f_S \rightarrow f$  as  $|D_j| \rightarrow 0$ , while the second one is the standard rule of importance sampling with  $N_{\alpha}$  discrete samples  $\{(\mathbf{x}_{\alpha}, \mathbf{k}_{\alpha})\}_{\alpha=1}^{N_{\alpha}}$  generated from the instrumental probability distribution  $f_I(\mathbf{x}, \mathbf{k}, t)$ , and the ‘weight’  $w_{\alpha}(t)$  reads

$$w_{\alpha}(t) = \frac{s_{\alpha}(t)}{\sum_{\alpha} s_{\alpha}(t)} \quad (89)$$

with

$$s_{\alpha}(t) = \frac{f_S(\mathbf{x}_{\alpha}, \mathbf{k}_{\alpha}, t)}{f_I(\mathbf{x}_{\alpha}, \mathbf{k}_{\alpha}, t) H(t)} \quad (90)$$

being either  $-1$  or  $1$  due to Eq. (87). In fact, the last approximation adopted in Eq. (88) implicitly utilizes the strong law of large number

$$\frac{1}{N_{\alpha}} \sum_{\alpha} H(t) s_{\alpha}(t) \rightarrow 1 \text{ as } N_{\alpha} \rightarrow +\infty, \quad a.s. \quad (91)$$

due to Eq. (84). It must be emphasized here that the sign function  $s_\alpha(t)$  indicates that every super-particle must be endowed with a sign, either positive or negative, for resolving the negative part of the Wigner distribution. Actually, the concept of signed particles, which emerges naturally here via the importance sampling, is the intrinsic feature of the Wigner Monte Carlo method, that is never seen in classical Vlasov or Boltzmann simulations.

However, the approximation (88) is rather formal since it requires the knowledge of  $f(\mathbf{x}, \mathbf{k}, t)$ , the solution of interest! By contrast, Eq. (70) provides a more convenient way to calculate  $\langle A \rangle_t$  in a time stepping manner. For the sake of brevity, we will divide the time interval  $[0, T]$  into  $n$  equidistant steps and denote  $t_l = l\Delta t, l = 1, 2, \dots, n$ , and  $\Delta t = T/n$ , though non-equidistant time steps are also allowed in principle. Besides, without loss of generality, we can take  $f(\mathbf{r}, \mathbf{k}, t_l)$  as the initial data and set the ending time to be  $t_{l+1}$ , owing to the Markovian property of the linear evolution system. Accordingly, based on Eq. (70), we can approximate  $\langle A \rangle_{t_{l+1}}$  through the principle of importance sampling as follows

$$\begin{aligned} \langle A \rangle_{t_{l+1}} &= \iint_{\mathbb{R}^d \times \mathcal{K}} \varphi(\mathbf{r}, \mathbf{k}, t_l) \cdot \frac{f(\mathbf{r}, \mathbf{k}, t_l)}{f_S(\mathbf{r}, \mathbf{k}, t_l)} \cdot \frac{f_S(\mathbf{r}, \mathbf{k}, t_l)}{f_I(\mathbf{r}, \mathbf{k}, t_l)} \cdot f_I(\mathbf{r}, \mathbf{k}, t_l) d\mathbf{r} d\mathbf{k} \\ &\approx \sum_{\alpha} \varphi(\mathbf{r}_{\alpha}, \mathbf{k}_{\alpha}, t_l) \cdot w_{\alpha}(t_l), \end{aligned} \quad (92)$$

where the discrete sample  $(\mathbf{r}_{\alpha}, \mathbf{k}_{\alpha})$ , generated from  $f_I(\mathbf{r}, \mathbf{k}, t_l)$ , corresponds to a super-particle located at  $(\mathbf{r}_{\alpha}, \mathbf{k}_{\alpha})$ , endowed with a signed weight of  $w_{\alpha}(t_l)$ . Consequently, it only remains to solve the adjoint equation with  $\varphi(\mathbf{r}, \mathbf{k}, t_{l+1}) = A(\mathbf{r}, \mathbf{k})$  to get  $\varphi(\mathbf{r}, \mathbf{k}, t_l)$  at several discrete samples  $(\mathbf{r}_{\alpha}, \mathbf{k}_{\alpha})$  via the branching process treatment discussed later. In particular, substituting  $A(\mathbf{r}, \mathbf{k}) = 1_{D_j}(\mathbf{r}, \mathbf{k})$  into Eq. (92) yields

$$\iint_{D_j} f(\mathbf{r}, \mathbf{k}, t_{l+1}) \approx \sum_{\alpha} \varphi(\mathbf{r}_{\alpha}, \mathbf{k}_{\alpha}, t_l) \cdot w_{\alpha}(t_l), \quad (93)$$

implying that we can readily attain the numerical solution  $f_S(\mathbf{r}, \mathbf{k}, t_{l+1})$  and the instrumental distribution  $f_I(\mathbf{r}, \mathbf{k}, t_{l+1})$  at the next time step.

More importantly, such a time marching scheme overcomes the intrinsic weakness of the branching process treatment, say, the exponential growth of particle number (see Theorem 6). Within each step, we only need to evolve the particle system for a relatively small  $\Delta t$  and update the instrumental distribution, from which we are able to draw new samples for the next loop. By exploiting the cancelation of weights of opposite sign, the resampling procedure can significantly reduce the particle number and save the computational efficiency dramatically in practice (See Section 7). Just because of such sampling reduction, the resampling procedure is also called *annihilation* in previous works, e.g., see [15].

The rest of this section is devoted to a computable, albeit not the unique, stochastic method for solving the adjoint equation based on the stochastic interpretation of its solution. In the subsequent sections, we will focus on the probabilistic approach for the adjoint equation (77), while all the deductions can be straightforwardly generalized to the Wigner equation due to the strong similarities between Eqs. (45) and (82).

## 5.2 A branching particle system

The remaining problem is to estimate  $\varphi(\mathbf{r}_\alpha, \mathbf{k}_\alpha, t_l)$  through  $A(\mathbf{r}, \mathbf{k})$ , as required in Eq. (92). The calculation can be realized by tracking the evolution of a branching particle system inherited in the renewal-type equation (82), which is described below in picturesque language using a branching particle system associated with an exit system. The exit system means that a particle in the branching system will be frozen when its life-length exceeds the final time  $T$ . All related rigorous analysis is left for the next subsection.

Consider a system of particles moving in  $\mathbb{R}^d \times \mathcal{K} \times [t, T]$  according to the following rules. Without loss of generality, the particle, starting at time  $t$  at state  $(\mathbf{r}, \mathbf{k})$ , having a random life-length  $\tau$  and carrying an initial weight  $\phi$ , is marked. The chosen initial data corresponds to those adopted in the renewal-type equation (82).

**Rule 1** The motion of each particle is described by a right continuous Markov process.

**Rule 2** The particle at  $(\mathbf{r}, \mathbf{k})$  dies in the age time interval  $(t, t')$  with probability  $\mathcal{G}(t'; \mathbf{r}, t)$ , which depends on its position  $\mathbf{r}$  and the time  $t$  (see Eq. (79)). In particular, when using the constant auxiliary function  $\gamma(x) \equiv \gamma_0$ , the particle dies during time interval  $(t, t')$  with probability  $1 - e^{-\gamma_0(t'-t)} \approx \gamma_0(t' - t)$  for small  $t' - t$ , which is totally independent of both its position and age.

**Rule 3** If  $t + \tau < T$ , the particle dies at age  $t' = t + \tau$  at state  $(\mathbf{r}(\tau), \mathbf{k})$ , and produces three new particles at states  $(\mathbf{r}'_{(1)}, \mathbf{k}'_{(1)})$ ,  $(\mathbf{r}'_{(2)}, \mathbf{k}'_{(2)})$ ,  $(\mathbf{r}'_{(3)}, \mathbf{k}'_{(3)})$ , endowed with updated weights  $\phi'_{(1)}$ ,  $\phi'_{(2)}$ ,  $\phi'_{(3)}$ , respectively. All these parameters can be determined by the kernel function in Eq. (82):

$$\begin{aligned} \frac{\Gamma(\mathbf{r}', \mathbf{k}'; \mathbf{r}(\tau), \mathbf{k})}{\gamma(\mathbf{r}(\tau))} &= \frac{\xi(\mathbf{r}')}{\gamma(\mathbf{r}(\tau))} \cdot \frac{V_w^-(\mathbf{r}', \mathbf{k} - \mathbf{k}')}{\xi(\mathbf{r}')} \cdot \delta(\mathbf{r}(\tau) - \mathbf{r}') \\ &\quad - \frac{\xi(\mathbf{r}')}{\gamma(\mathbf{r}(\tau))} \cdot \frac{V_w^+(\mathbf{r}', \mathbf{k} - \mathbf{k}')}{\xi(\mathbf{r}')} \cdot \delta(\mathbf{r}(\tau) - \mathbf{r}') \\ &\quad + 1 \cdot \delta(\mathbf{k} - \mathbf{k}') \cdot \delta(\mathbf{r}(\tau) - \mathbf{r}'), \end{aligned} \quad (94)$$

and thus

$$\mathbf{r}'_{(1)} = \mathbf{r}'_{(2)} = \mathbf{r}'_{(3)} = \mathbf{r}(\tau), \quad (95)$$

$$\mathbf{k} - \mathbf{k}'_{(1)} \propto \frac{V_w^-(\mathbf{r}(\tau), \mathbf{k})}{\xi(\mathbf{r}(\tau))}, \quad \mathbf{k} - \mathbf{k}'_{(2)} \propto \frac{V_w^+(\mathbf{r}(\tau), \mathbf{k})}{\xi(\mathbf{r}(\tau))}, \quad \mathbf{k}'_{(3)} = \mathbf{k}, \quad (96)$$

$$\phi'_{(1)} = \zeta(\mathbf{r}(\tau)) \cdot \phi, \quad \phi'_{(2)} = -\zeta(\mathbf{r}(\tau)) \cdot \phi, \quad \phi'_{(3)} = 1 \cdot \phi, \quad (97)$$

where the function  $\xi(\mathbf{r})$  is the normalization factor for both  $V_w^+$  and  $V_w^-$ , i.e.,

$$\xi(\mathbf{r}) = \int_{2\mathcal{K}} V_w^+(\mathbf{r}, \mathbf{k}) d\mathbf{k} = \int_{2\mathcal{K}} V_w^-(\mathbf{r}, \mathbf{k}) d\mathbf{k}, \quad (98)$$

because of the mass conservation (19), and

$$\zeta(\mathbf{r}) = \frac{\xi(\mathbf{r})}{\gamma(\mathbf{r})}. \quad (99)$$

Actually, besides Eq. (96), it is required that both  $\mathbf{k}'_{(1)} \in \mathcal{K}$  and  $\mathbf{k}'_{(2)} \in \mathcal{K}$  hold, otherwise  $\mathbf{k}'_{(1)}$  and  $\mathbf{k}'_{(2)}$  must be rejected.

**Rule 4** If  $t + \tau \geq T$ , say, the life-length of the particle exceeds  $T - t$ , it will immigrate to the state  $(\mathbf{r}(T - t), \mathbf{k})$  and be frozen. This rule corresponds to the first right-hand-side term of Eq. (82), and the related probability is

$$\Pr(\tau \geq T - t) = 1 - \mathcal{G}(T; \mathbf{r}, t) = \mathbb{e}^{-\int_t^T \gamma(\mathbf{r}(s-t))ds}. \quad (100)$$

**Rule 5** The only interaction between the particles is that the birth time and state of offsprings coincide with the death time and state of their parent.

Based on the above five rules, we can establish the framework of the branching process to calculate numerically the Wigner function in the following three steps, e.g., from  $t_l$  to  $t_{l+1}$  with the time step  $\Delta t$ ,  $l = 1, 2, \dots, n - 1$ . Recall that we would like to estimate  $\varphi(\mathbf{r}_\alpha, \mathbf{k}_\alpha, t_l)$ , thus it suffices to take  $\mathbf{r} = \mathbf{r}_\alpha, \mathbf{k} = \mathbf{k}_\alpha, t = t_l$  (i.e., the initial state), and  $\mathbf{r}' = \mathbf{r}'_\alpha, \mathbf{k}' = \mathbf{k}'_\alpha, t' = t'_\alpha$  for the offsprings in Eq. (82).

**Step 1: Sample from the instrumental distribution** The first step is to sample  $N_\alpha$  ancestor particles according to the instrumental distribution  $f_I(\mathbf{r}, \mathbf{k}, t_l)$  (see Eq. (85)). Each particle has a state  $(\mathbf{r}_\alpha, \mathbf{k}_\alpha)$  and carries a weight  $\phi_\alpha$ .

**Step 2: Evolve the particles** The second step is to evolve super-particles according to the rules of branching particle systems. Suppose a particle is born at  $t'_\alpha \in [t_l, t_{l+1}]$  at state  $(\mathbf{r}'_\alpha, \mathbf{k}'_\alpha)$  with weight  $\phi'_\alpha$ , and it has a random life-length  $\tau'_\alpha$  satisfying

$$\tau'_\alpha \propto \left. \frac{d\mathcal{G}(t'; \mathbf{r}'_\alpha, t'_\alpha)}{dt'} \right|_{t'=t'_\alpha+\tau'_\alpha} = \gamma(\mathbf{r}'_\alpha(\tau'_\alpha)) \mathbb{e}^{-\int_{t'_\alpha}^{t'_\alpha+\tau'_\alpha} \gamma(\mathbf{r}'_\alpha(s-t'_\alpha))ds}. \quad (101)$$

When  $t'_\alpha = t_l$ ,  $(\mathbf{r}'_\alpha, \mathbf{k}'_\alpha) = (\mathbf{r}_\alpha, \mathbf{k}_\alpha)$ ,  $\phi'_\alpha = \phi_\alpha$ , it indicates that such a particle is an ancestor in Step 1.

If  $\tau'_\alpha \geq t_{l+1} - t'_\alpha$ , the particle is frozen at the state  $(\mathbf{r}'_\alpha(t_{l+1} - t'_\alpha), \mathbf{k}'_\alpha)$  and the probability of this event is

$$\Pr(\tau'_\alpha \geq t_{l+1} - t'_\alpha) = 1 - \mathcal{G}(t_{l+1}; \mathbf{r}'_\alpha, t'_\alpha) = \mathbb{e}^{-\int_{t'_\alpha}^{t_{l+1}} \gamma(\mathbf{r}'_\alpha(s-t'_\alpha))ds}. \quad (102)$$

Otherwise, the particle travels to a new position  $\mathbf{r}'_\alpha(\tau'_\alpha)$  and dies at time  $t'_\alpha + \tau'_\alpha$  at state  $(\mathbf{r}'_\alpha(\tau'_\alpha), \mathbf{k}'_\alpha)$ , and meanwhile, three new particles are generated according to Rule 3, the probability of which is  $\mathcal{G}(t'_\alpha + \tau'_\alpha; \mathbf{r}'_\alpha, t'_\alpha)$ .

**Step 3: Update the Wigner function** When all particles in the branching system are frozen, we need to record their positions, wavevectors, and weights. Let  $\mathcal{E}_\alpha$  denote the index set of all frozen particles with the same ancestor initially at state  $(\mathbf{r}_\alpha, \mathbf{k}_\alpha)$ ,  $\{(\mathbf{r}_{i,\alpha}, \mathbf{k}_{i,\alpha}), i \in \mathcal{E}_\alpha\}$  the collection of corresponding frozen states, and  $\phi_{i,\alpha}$  the updated weight of the  $i$ -th particle. Accordingly, the adjoint variable can be approximated as

$$\varphi(\mathbf{r}_\alpha, \mathbf{k}_\alpha, t_l) \approx \sum_{i \in \mathcal{E}_\alpha} \phi_{i,\alpha} \cdot A(\mathbf{r}_{i,\alpha}, \mathbf{k}_{i,\alpha}), \quad (103)$$

and substituting it into Eq. (92) leads to

$$\langle A \rangle_{t_{l+1}} \approx \sum_{\alpha} \sum_{i \in \mathcal{E}_\alpha} \phi_{i,\alpha} \cdot w_\alpha(t_l) \cdot A(\mathbf{r}_{i,\alpha}, \mathbf{k}_{i,\alpha}). \quad (104)$$

Particularly, plugging into  $A(\mathbf{r}, \mathbf{k}) = 1_{D_j}(\mathbf{r}, \mathbf{k})$ , we obtain  $f_S(\mathbf{r}, \mathbf{k}, t_{l+1})$  from Eq. (93), which not only serves as an estimator to the Wigner distribution  $f(\mathbf{r}, \mathbf{k}, t_{l+1})$ , but also renders the instrumental distribution  $f_I(\mathbf{r}, \mathbf{k}, t_{l+1})$  required in the next loop. After that, we return to the first step, resample from the updated instrumental distribution and continue until the final time  $T$  is reached. In practice, the resampling leads to a sharp decrease of particles in the branching particle system (see Sections 6.4 and 7).

So far we have avoided the rigorous deduction and only depicted an intuitive picture of the branching particle system. But it naturally arouses two questions below.

**Question 1** Does the approximation (104) really converge?

**Question 2** How to estimate the growth rate of particle number?

To solve Question 1, a validation of the probabilistic approach through stochastic analysis is required. For Question 2, we recourse to the theory of branching process. Actually, the answer to Question 2 is extremely important in real applications because of the limited computational resource. We expect to give a reliable criterion on how to suppress the growth of particle number in numerical simulations.

### 5.3 Stochastic interpretation

In the theory of branching process, all the moments of an age-dependent branching processes satisfy renewal-type integral equations [32], where the term “age-dependent” means the probability that a particle, living at  $t$ , dies at  $(t, t + \Delta t)$  might not be a constant function of  $t$ . In this regard, it suffices to define a stochastic branching Markov process (continuous in time parameter), corresponding to the branching particle system as described before.

The random variable of a branching particle system is the family history, a denumerable random sequence corresponding to a unique family tree. Firstly, we

need a sequence to identify the objects in a family. Beginning with an ancestor, denoted by  $\langle 0 \rangle$ , and we can denote its first, second and third children by  $\langle 1 \rangle$ ,  $\langle 2 \rangle$ ,  $\langle 3 \rangle$ . Similarly, we can denote the  $j$ -th child of  $i$ -th child by  $\langle ij \rangle$ , and thus  $\langle i_1 i_2 \cdots i_n \rangle$  means  $i_n$ -th child of  $i_{n-1}$ -th child of  $\cdots$  of the  $i_2$ -child of the  $i_1$ -th child, with  $i_n \in \{1, 2, 3\}$ . The ancestor  $\langle 0 \rangle$  is omitted here and hereafter for brevity.

Our branching particle system involves three basic elements: the position  $\mathbf{r}$  (or  $\mathbf{x}$ ), the wavevector  $\mathbf{k}$  and the life-length  $\tau$ , and each particle will either immigrate to  $\mathbf{r}(\tau) = \mathbf{r} + \hbar \mathbf{k} \tau / m$ , then be killed and produce three offsprings, or be frozen when hitting the first exit time  $T$ . Now we can give the definition of a family history, starting from one particle at age  $t$  at state  $(\mathbf{r}, \mathbf{k})$ . In the subsequent discussion we let  $(\mathbf{r}_0, \mathbf{k}_0) = (\mathbf{r}, \mathbf{k})$ .

**Definition 1.** A family history  $\omega$  stands for a random sequence

$$\omega = ((\tau_0, \mathbf{r}_0, \mathbf{k}_0); (\tau_1, \mathbf{r}_1, \mathbf{k}_1); (\tau_2, \mathbf{r}_2, \mathbf{k}_2); (\tau_3, \mathbf{r}_3, \mathbf{k}_3); (\tau_{11}, \mathbf{r}_{11}, \mathbf{k}_{11}); \cdots), \quad (105)$$

where the tuple  $Q_i = (\tau_i, \mathbf{r}_i, \mathbf{k}_i)$  appears in a definite order of enumeration.  $\tau_i$ ,  $\mathbf{r}_i$ ,  $\mathbf{k}_i$  denote the life-length, starting position and wavevector of the  $i$ -th particle, respectively. The exact order of  $Q_i$  is immaterial but is supposed to be fixed. The collection of all family histories is denoted by  $\Omega$ .

At this stage, the initial time  $t$  and the initial state  $(\mathbf{r}_0, \mathbf{k}_0)$  of the ancestor particle  $\langle 0 \rangle$  are assumed to be non-stochastic.

**Definition 2.** For each  $\omega = (Q_0; Q_1; Q_2; Q_3; Q_{11} \cdots)$ , the subfamily  $\omega_i$  is the family history of  $\langle i \rangle$  and its descendants, defined by  $\omega_i = (Q_i; Q_{i1}; Q_{i2}; Q_{i3}; \cdots)$ . The collection of  $\omega_i$  is denoted by  $\Omega_i$ .

Equivalently, we can also use the time parameter to identify the path of a particle and all its ancestors in the family history, and denote  $\eta_s$  its state (i.e., starting position and wavevector) at time  $s \geq t$ . Taking the particle  $i = \langle i_1 i_2 \cdots \rangle$  as an example, we have  $Q_0 = (\tau_0, \eta_t)$  with  $\eta_t = (\mathbf{r}_0, \mathbf{k}_0)$ ,  $Q_{i_1} = (\tau_{i_1}, \eta_{t_{i_1}})$  with  $t_{i_1} = t + \tau_0$  and  $\eta_{t_{i_1}} = (\mathbf{r}_{i_1}, \mathbf{k}_{i_1})$ ,  $Q_{i_1 i_2} = (\tau_{i_1 i_2}, \eta_{t_{i_1 i_2}})$  with  $t_{i_1 i_2} = t_{i_1} + \tau_{i_1}$  and  $\eta_{t_{i_1 i_2}} = (\mathbf{r}_{i_1 i_2}, \mathbf{k}_{i_1 i_2})$ ,  $\cdots$ . To characterize the freezing behavior of the particle, we denote the first exit time by  $T$ , as boundary conditions are not specified.

**Definition 3.** Suppose the family history starts at time  $t$ . Then a particle  $\langle i_1 i_2 \cdots i_n \rangle$  is said to be frozen at  $T$  if the following conditions hold

$$t + \tau_0 + \tau_{i_1} + \tau_{i_1 i_2} + \cdots + \tau_{i_1 i_2 \cdots i_{n-1}} < T, \quad (106)$$

$$t + \tau_0 + \tau_{i_1} + \tau_{i_1 i_2} + \cdots + \tau_{i_1 i_2 \cdots i_{n-1}} + \tau_{i_1 i_2 \cdots i_n} \geq T. \quad (107)$$

In particular, when  $t + \tau_0 \geq T$ , the ancestor particle  $\langle 0 \rangle$  is frozen. Sometimes the particle  $\langle i_1 i_2 \cdots i_n \rangle$  is also called alive in the time interval  $[t, T]$ . The collection of frozen particles is denoted by  $\mathcal{E}(\omega)$ .

**Remark 1.** The first exit time  $\tau_e(O)$  from an open set  $O$  is defined by

$$\tau_e(O) = \inf \{s \geq t : (s, \eta_s) \notin O\}.$$

Since a boundary condition is not applied yet, we have  $O = (-\infty, T) \times \mathbb{R}^d \times \mathcal{K}'$  with  $\mathcal{K}'$  being an open cover of  $\mathcal{K}$ , and thus  $\tau_e(O) = T$ .

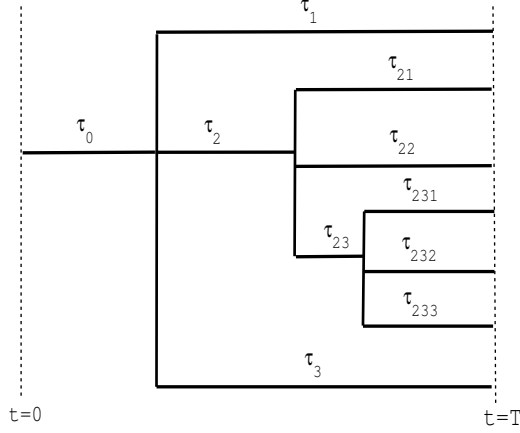


Figure 1: An example of family history tree.

**Example 1.**  $\omega = (Q_0; Q_1; Q_2; Q_3; Q_{21}; Q_{22}; Q_{23}; Q_{231}; Q_{232}; Q_{233})$  uniquely determines a family history tree, as shown in Fig. 1.  $\omega_2 = (Q_2; Q_{21}; Q_{22}; Q_{23}; Q_{231}; Q_{232}; Q_{233})$  is a subfamily history that describes the family history of  $Q_2$  and its descendants, and we have  $\omega = (Q_0; \omega_1; \omega_2; \omega_3)$ . The collection of frozen particles is  $\mathcal{E}(\omega) = \{\langle 1 \rangle, \langle 21 \rangle, \langle 22 \rangle, \langle 231 \rangle, \langle 232 \rangle, \langle 233 \rangle, \langle 3 \rangle\}$ .

Hereafter we assume that all particles in the branching particle system will move until reaching the frozen state, and still use  $\Omega$  to denote the collection of the family history of all frozen particles. Now we need to define a probability measure  $\Pi_{t, \mathbf{r}, \mathbf{k}}$  on  $\Omega$ , corresponding to the branching process started from state  $(\mathbf{r}, \mathbf{k})$  at time  $t$ .

For the Borel sets  $T_i \subset [0, +\infty)$  ( $i = 0, 1, \dots, n$ ),  $R_i \subset \mathbb{R}^d$ ,  $K_i \subset \mathcal{K}$  ( $i = 1, 2, \dots, n$ ) on  $\Omega$ , let  $E = \{\tau_0 \in T_0, (\tau_{i_1}, \eta_{t_{i_1}}) \in T_1 \times R_1 \times K_1, \dots, (\tau_{i_1 i_2 \dots i_n}, \eta_{t_{i_1 i_2 \dots i_n}}) \in T_n \times R_n \times K_n\}$ , then the probability of the event  $E$  is

$$\begin{aligned}
\Pr(E) &= \int_{T_0} d\tau_0 \cdots \int_{T_n} d\tau_{i_1 i_2 \dots i_n} \int_{R_1} d\mathbf{r}_{i_1} \int_{K_1} d\mathbf{k}_{i_1} \cdots \int_{R_n} d\mathbf{r}_{i_1 i_2 \dots i_n} \int_{K_n} d\mathbf{k}_{i_1 i_2 \dots i_n} \\
&\quad \times p_{i_1}(t, \mathbf{r}_0, \mathbf{k}_0; t_{i_1}, \mathbf{r}_{i_1}, \mathbf{k}_{i_1}) \times p_{i_2}(t_{i_1}, \mathbf{r}_{i_1}, \mathbf{k}_{i_1}; t_{i_1 i_2}, \mathbf{r}_{i_1 i_2}, \mathbf{k}_{i_1 i_2}) \times \cdots \\
&\quad \times p_{i_n}(t_{i_1 i_2 \dots i_{n-1}}, \mathbf{r}_{i_1 i_2 \dots i_{n-1}}, \mathbf{k}_{i_1 i_2 \dots i_{n-1}}; t_{i_1 i_2 \dots i_n}, \mathbf{r}_{i_1 i_2 \dots i_n}, \mathbf{k}_{i_1 i_2 \dots i_n}) \\
&\quad \times p(t_{i_1 i_2 \dots i_n}, \mathbf{r}_{i_1 i_2 \dots i_n}; t_{i_1 i_2 \dots i_n} + \tau_{i_1 i_2 \dots i_n})
\end{aligned} \tag{108}$$

with  $i_l \in \{1, 2, 3\}$  ( $l = 1, 2, \dots, n$ ). Here the transition densities  $p_{i_l}$  and  $p$  are given

by

$$p_1(t, \mathbf{r}, \mathbf{k}; t', \mathbf{r}', \mathbf{k}') = p(t, \mathbf{r}; t') \cdot \frac{V_w^-(\mathbf{r}', \mathbf{k} - \mathbf{k}') \cdot 1_{\{\mathbf{k}' \in \mathcal{K}\}}}{\xi(\mathbf{r}')} \cdot \delta(\mathbf{r}' - \mathbf{r}(\tau)), \quad (109)$$

$$p_2(t, \mathbf{r}, \mathbf{k}; t', \mathbf{r}', \mathbf{k}') = p(t, \mathbf{r}; t') \cdot \frac{V_w^+(\mathbf{r}', \mathbf{k} - \mathbf{k}') \cdot 1_{\{\mathbf{k}' \in \mathcal{K}\}}}{\xi(\mathbf{r}')} \cdot \delta(\mathbf{r}' - \mathbf{r}(\tau)), \quad (110)$$

$$p_3(t, \mathbf{r}, \mathbf{k}; t', \mathbf{r}', \mathbf{k}') = p(t, \mathbf{r}; t') \cdot \delta(\mathbf{k} - \mathbf{k}') \cdot \delta(\mathbf{r}' - \mathbf{r}(\tau)), \quad (111)$$

$$p(t, \mathbf{r}; t') = \left. \frac{d\mathcal{G}(t'; \mathbf{r}, t)}{dt'} \right|_{t'=t+\tau}, \quad (112)$$

where  $\mathcal{G}(t'; \mathbf{r}, t)$  has been defined in Eq. (79) and the stochastic life time  $\tau = t' - t$  is chosen according to  $\tau \propto p(t, \mathbf{r}; t')$ . Combining with the independence assumption in Rule 5, we are able to define a probability measure  $\Pi_{t, \mathbf{r}, \mathbf{k}}$  on  $\Omega$  as follows

$$\Pi_{t, \mathbf{r}, \mathbf{k}}(1_E) = \int_{\Omega} 1_E(\omega) \Pi_{t, \mathbf{r}, \mathbf{k}}(d\omega) = \Pr(E), \quad (113)$$

as well as a stochastic branching process  $(\Omega, \Pi_{t, \mathbf{r}, \mathbf{k}})$ . Moreover, from Eq. (108), we can easily verify the following Markov property of the stochastic process  $(\Omega, \Pi_{t, \mathbf{r}, \mathbf{k}})$

$$\Pi_{t, \mathbf{r}, \mathbf{k}}(XY) = \int_{\Omega_X} X \Pi_{t+\tau, \eta_{t+\tau}}(Y) \Pi_{t, \mathbf{r}, \mathbf{k}}(d\omega) \quad (114)$$

for any function  $X$  in a measurable space  $(\Omega_X, \mathcal{T}_{[t, t+\tau]} \otimes \mathcal{F}_{[t, t+\tau]})$  and any function  $Y$  in  $(\Omega_Y, \mathcal{T}_{[t+\tau, +\infty)} \otimes \mathcal{F}_{[t+\tau, T]})$ , where  $\mathcal{T}_{\mathcal{I}}$  is the  $\sigma$ -algebra on  $\mathcal{I} \subset [0, +\infty)$ ,  $\mathcal{F}_{\mathcal{I}}$  is the  $\sigma$ -algebra generated by  $\eta_s$  with  $s \in \mathcal{I}$ , and  $\Omega = \Omega_X \times \Omega_Y$ . That is, *events observable before and after time  $t + \tau$  are conditionally independent for given state  $\eta_{t+\tau}$ .*

**Remark 2.** Since  $\omega \in \Omega$  corresponds to a denumerable random sequence, the basic theorem of Kolmogorov (see Theorem 6.16, [33]) ensures the existence and uniqueness of such a random process  $(\Omega, \mathcal{B}_{\Omega}, \Pi_{t, \mathbf{r}, \mathbf{k}})$  with the probability measure  $\Pi_{t, \mathbf{r}, \mathbf{k}}$  defined on the Borel extension  $\mathcal{B}_{\Omega}$  of the cylinder sets on  $\Omega$  [32].

Next we need to define a random measure  $\mu : (\mathbb{R}^d \times \mathcal{K}, \mathcal{B}) \rightarrow \mathbb{R}$  through the particle weights and the frozen states, where  $\mathcal{B} \in \mathcal{B}_{\Omega}$  and  $\mathcal{B}_{\Omega}$  stands for the Borel cylinder sets on  $\Omega$ . According to Rule 4, the frozen state of a particle  $\langle i_1 i_2 \cdots i_n \rangle$  is  $(\mathbf{r}_{i_1 i_2 \cdots i_n}(T - t_{i_1 i_2 \cdots i_n}), \mathbf{k}_{i_1 i_2 \cdots i_n})$  with  $t_{i_1 i_2 \cdots i_n} = t + \tau_0 + \cdots + \tau_{i_1 i_2 \cdots i_{n-1}}$ , and the frozen state of  $\langle 0 \rangle$  is  $(\mathbf{r}_0(T - t), \mathbf{k}_0)$ .

**Definition 4.** Suppose  $(\mathbf{r}_i, \mathbf{k}_i)$  is the starting state of a frozen particle  $i$  in a given family history  $\omega$ , and let  $\delta_{(\mathbf{r}, \mathbf{k})}$  mean the unit measure concentrated at state  $(\mathbf{r}, \mathbf{k})$ . Then we define the exit measure as follows

$$\mu = \sum_{i \in \mathcal{E}(\omega)} \phi_i \cdot \delta_{(\mathbf{r}_i(T - t_i), \mathbf{k}_i)}, \quad (115)$$

where  $\phi_i$  is the cumulative weight of particle  $i$ . For an object  $i = \langle i_1 i_2 \cdots i_n \rangle$ ,  $\phi_i$  is given by

$$\phi_i = \phi \cdot \zeta(\mathbf{r}_{i_1}) \cdot \zeta(\mathbf{r}_{i_1 i_2}) \cdots \zeta(\mathbf{r}_{i_1 i_2 \cdots i_{n-1}}), \quad (116)$$



where  $\phi$  is the initial weight of the ancestor and the function  $\zeta(\mathbf{r})$  has been defined in Eq. (99). Moreover, for given  $\omega$  and function  $A(\mathbf{r}, \mathbf{k})$ , we can further define a random integral on the point distribution

$$\mu_A(\omega) = \int A(\mathbf{r}, \mathbf{k}) \mu(d\mathbf{r} \times d\mathbf{k}, \omega) = \sum_{i \in \mathcal{E}(\omega)} \phi_i \cdot A(\mathbf{r}_i(T - t_i), \mathbf{k}_i). \quad (117)$$

To ensure a bounded weight, we require  $|\zeta(\mathbf{r})| \leq 1$  for any  $\mathbf{r} \in \mathbb{R}^d$ . The first moment of random function  $\mu_A(\omega)$  is denoted by  $\psi(\mathbf{r}, \mathbf{k}, t)$  which reads

$$\psi(\mathbf{r}, \mathbf{k}, t) = \Pi_{t, \mathbf{r}, \mathbf{k}}(\mu_A) = \int_{\Omega} \mu_A(\omega) \Pi_{t, \mathbf{r}, \mathbf{k}}(d\omega). \quad (118)$$

**Example 2.** Suppose the initial weight  $\phi = 1$  at  $t = 0$ . For the family history  $\omega$  displayed in Fig. 1, the random integral  $\mu_A(\omega)$  is

$$\begin{aligned} \mu_A(\omega) = & \zeta(\mathbf{r}_1)A(\mathbf{r}_1(T - \tau_0), \mathbf{k}_1) + \zeta(\mathbf{r}_2)\zeta(\mathbf{r}_{21})A(\mathbf{r}_{21}(T - \tau_0 - \tau_2), \mathbf{k}_{21}) \\ & + \zeta(\mathbf{r}_2)\zeta(\mathbf{r}_{22})A(\mathbf{r}_{22}(T - \tau_0 - \tau_2), \mathbf{k}_{22}) \\ & + \zeta(\mathbf{r}_2)\zeta(\mathbf{r}_{23})\zeta(\mathbf{r}_{231})A(\mathbf{r}_{231}(T - \tau_0 - \tau_2 - \tau_{23}), \mathbf{k}_{231}) \\ & + \zeta(\mathbf{r}_2)\zeta(\mathbf{r}_{23})\zeta(\mathbf{r}_{232})A(\mathbf{r}_{232}(T - \tau_0 - \tau_2 - \tau_{23}), \mathbf{k}_{232}) \\ & + \zeta(\mathbf{r}_2)\zeta(\mathbf{r}_{23})\zeta(\mathbf{r}_{233})A(\mathbf{r}_{233}(T - \tau_0 - \tau_2 - \tau_{23}), \mathbf{k}_{233}) \\ & + \zeta(\mathbf{r}_3)A(\mathbf{r}_3(T - \tau_0), \mathbf{k}_3). \end{aligned} \quad (119)$$

In order to study the particle number in the branching particle system with the family history  $\omega$  starting from time  $t$ , we use a random function  $Z(\omega, T - t)$  to stand for the total number of frozen particles at the final instant  $T$ . In consequence, the first moment of  $Z(\omega, T - t)$  is

$$M(T - t) = \int_{\Omega} Z(\omega, T - t) \Pi_{t, \mathbf{r}, \mathbf{k}}(d\omega), \quad (120)$$

which also gives the expectation of the total number of alive particles in time interval  $[t, T]$ , and should be finite (see Theorem 3). This further means that  $Z(\omega, T - t)$  is finite almost surely. As the easier case, the finiteness of  $M(T - t)$  for the constant auxiliary function is directly implied from Theorem 13.1 and its corollary of Chapter VI in [32].

**Theorem 3.** Suppose the family history  $\omega$  starts at time  $t$  at state  $(\mathbf{r}, \mathbf{k})$ , and ends at  $T$ . Then  $M(T - t) < \infty$  and as a consequence  $\Pr(\{Z(\omega, T - t) < \infty\}) = 1$ .

*Proof.* We define a random function  $1_{i_1 i_2 \dots i_n}(\omega) = 1$  when the particle  $\langle i_1 i_2 \dots i_n \rangle$  appears in the family history  $\omega$ , otherwise  $1_{i_1 i_2 \dots i_n}(\omega) = 0$ . From Eq. (113) and Definition 3, we have

$$\Pi_{t, \mathbf{r}, \mathbf{k}}(1_{i_1 i_2 \dots i_n}) = \int_{\Omega} 1_{i_1 i_2 \dots i_n}(\omega) \Pi_{t, \mathbf{r}, \mathbf{k}}(d\omega) = \Pr(\{t + \tau_0 + \dots + \tau_{i_1 i_2 \dots i_{n-1}} < T\}). \quad (121)$$

Let

$$\bar{Z}(\omega, T-t) = 1 + \sum_{n=1}^{\infty} \sum_{i_1, \dots, i_n=1}^3 1_{i_1 i_2 \dots i_n}(\omega), \quad (122)$$

that corresponds to the number of particles born up to the final time  $T$ . It is obvious that

$$Z(\omega, T-t) \leq \bar{Z}(\omega, T-t). \quad (123)$$

For constant  $\gamma_0$ , we introduce an exponential distribution

$$G(t') = 1 - e^{-\gamma_0(t'-t)}, \quad t' \geq t, \quad (124)$$

and define its  $n$ -th convolution by

$$G_0(t') = G(t'), \quad G_n(t') = \int_0^{t'} G_{n-1}(t' - u) dG(u). \quad (125)$$

It can be readily verified that

$$\frac{d\mathcal{G}(t'; \mathbf{r}, u)}{dt'} \leq \frac{k}{3} \cdot \frac{dG(t')}{dt'}, \quad \forall t' \in [u, T], \quad \forall \mathbf{r} \in \mathbb{R}^d, \quad \forall u \in [0, T], \quad (126)$$

holds for a sufficiently large integer  $k$ , e.g.,  $k > 3e^{\gamma_0 T}$ .

We first show by the mathematical induction that there exists a sufficient large integer  $k$  and a sufficient large constant  $\gamma_0 > 0$  such that

$$\Pr(\{t + \tau_0 + \dots + \tau_{i_1 i_2 \dots i_{n-1}} < T - u\}) \leq \left(\frac{k}{3}\right)^{n-1} G_{n-1}(T - u), \quad \forall u \in [0, T - t]. \quad (127)$$

For  $n = 1$ , we only need  $\gamma_0 \geq \max\{\gamma(\mathbf{r})\}$  and then have

$$\begin{aligned} \Pr(\{t + \tau_0 < T - u\}) &= \left. \frac{d\mathcal{G}(t'; \mathbf{r}, t)}{dt'} \right|_{t'=T-u} = 1 - e^{-\int_t^{T-u} \gamma(\mathbf{r}(s-t)) ds} \\ &\leq 1 - e^{-\gamma_0(T-u-t)} = G_0(T - u). \end{aligned} \quad (128)$$

Assume Eq. (127) is true for  $n$ . Direct calculation shows

$$\begin{aligned} \Pr(\{t + \tau_0 + \dots + \tau_{i_1 i_2 \dots i_n} < T - u\}) &= \Pi_{t, \mathbf{r}, \mathbf{k}}(1_{\{t + \tau_0 + \dots + \tau_{i_1 i_2 \dots i_n} < T - u\}}) \\ &= \int_0^{T-t-u} \Pi_{t, \mathbf{r}, \mathbf{k}}(1_{\{t + \tau_0 + \dots + \tau_{i_1 i_2 \dots i_{n-1}} < T - u - v\}} 1_{\{\tau_{i_1 i_2 \dots i_n} < v\}}) dv \\ &= \int_0^{T-t-u} \Pi_{t, \mathbf{r}, \mathbf{k}}(1_{\{t + \tau_0 + \dots + \tau_{i_1 i_2 \dots i_{n-1}} < T - u - v\}} \cdot \Pi_{\sigma, \eta_\sigma}(1_{\{\tau_{i_1 i_2 \dots i_n} < v\}})) dv \\ &\leq \int_0^{T-t-u} \left(\frac{k}{3}\right)^{n-1} G_{n-1}(T - u - v) \cdot \frac{k}{3} dG(v) = \left(\frac{k}{3}\right)^n G_n(T - u), \end{aligned} \quad (129)$$

which implies that Eq. (127) holds for  $n+1$ , where  $\sigma$  is short for  $t + \tau_0 + \dots + \tau_{i_1 i_2 \dots i_{n-1}}$ .

Finally, using Eqs. (121) and (127) yields

$$\int_{\Omega} \bar{Z}(\omega, T-t) \Pi_{t, \mathbf{r}, \mathbf{k}}(d\omega) = 1 + \sum_{n=1}^{\infty} \sum_{i_1, \dots, i_n=1}^3 \Pi_{t, \mathbf{r}, \mathbf{k}}(1_{i_1 i_2 \dots i_n}) \leq 1 + 3 \sum_{n=1}^{\infty} k^{n-1} G_{n-1}(T),$$

and implies  $\int_{\Omega} \bar{Z}(\omega, T-t) \Pi_{t,\mathbf{r},\mathbf{k}}(d\omega)$  is bounded for the infinite series is convergent (see Lemma 1 of the Appendix to Chapter VI in [32]). Hence the proof is completed according to Eq. (123).  $\square$

Moreover, according to Definition 4 and Theorem 3, we can directly show the  $L^1$ -convergence of  $\mu_A$ , say,

$$\int_{\Omega} |\mu_A(\omega)| \Pi_{t,\mathbf{r},\mathbf{k}}(d\omega) < \infty, \quad (130)$$

provided that  $A(\mathbf{r}, \mathbf{k})$  is bounded. That is, both  $\mu_A$  in Eq. (117) and  $\psi$  in Eq. (118) are well defined.

After finishing the above preparations, we begin to answer the questions raised in the end of Section 5.2. Theorem 4 tries to answer Question 1, while the answer for Question 2 is given in Theorem 6.

**Theorem 4.** *The first moment  $\psi(\mathbf{r}, \mathbf{k}, t)$  defined in Eq. (118) happens to be a solution of the adjoint equation (77).*

*Proof.* Let  $E = \{\tau_0 : t + \tau_0 \geq T\} \cap \Omega$  correspond to the case in which the particle travels to  $(\mathbf{r}(T-t), \mathbf{k})$  and then is frozen. The probability of such event is  $1 - \mathcal{G}(T; \mathbf{r}, t)$  by Rule 4. Then the remaining case is denoted by  $E^c = \{\tau_0 : t + \tau_0 < T\} \cap \Omega$ . Accordingly, from Eq. (118), we have

$$\psi(\mathbf{r}, \mathbf{k}, t) = \int_E \mu_A(\omega) \Pi_{t,\mathbf{r},\mathbf{k}}(d\omega) + \int_{E^c} \mu_A(\omega) \Pi_{t,\mathbf{r},\mathbf{k}}(d\omega), \quad (131)$$

and direct calculation gives

$$\int_E \mu_A(\omega) \Pi_{t,\mathbf{r},\mathbf{k}}(d\omega) = e^{-\int_t^T \gamma(\mathbf{r}(s-t)) ds} A(\mathbf{r}(T-t), \mathbf{k}), \quad (132)$$

which recovers the first right-hand-side term of Eq. (77). When event  $E^c$  occurs, it indicates that three offsprings are generated. Notice that  $\omega = (Q_0; \omega_1; \omega_2; \omega_3)$  and thus we have

$$\begin{aligned} \mu_A(\omega) &= \phi_1 \cdot \mu_A(\omega_1) + \phi_2 \cdot \mu_A(\omega_2) + \phi_3 \cdot \mu_A(\omega_3), \\ &= \zeta(\mathbf{r}(\tau_0)) \cdot \mu_A(\omega_1) - \zeta(\mathbf{r}(\tau_0)) \cdot \mu_A(\omega_2) + \mu_A(\omega_3), \end{aligned} \quad (133)$$

where we have applied Rule 3 and set the initial weight  $\phi = 1$  for simplicity.

Substitute Eq. (133) into the second right-hand-side term of Eq. (131) leads to

$$\begin{aligned} \int_{E^c} \mu_A(\omega) \Pi_{t,\mathbf{r},\mathbf{k}}(d\omega) &= \int_{E^c} \zeta(\mathbf{r}(\tau_0)) \left\{ \int_{\Omega_1} \mu_A(\omega_1) \Pi_{t+\tau_0, \mathbf{r}_1, \mathbf{k}_1}(d\omega_1) \right\} \Pi_{t,\mathbf{r},\mathbf{k}}(d\omega) \\ &\quad - \int_{E^c} \zeta(\mathbf{r}(\tau_0)) \left\{ \int_{\Omega_2} \mu_A(\omega_2) \Pi_{t+\tau_0, \mathbf{r}_2, \mathbf{k}_2}(d\omega_2) \right\} \Pi_{t,\mathbf{r},\mathbf{k}}(d\omega) \\ &\quad + \int_{E^c} \left\{ \int_{\Omega_3} \mu_A(\omega_3) \Pi_{t+\tau_0, \mathbf{r}_3, \mathbf{k}_3}(d\omega_3) \right\} \Pi_{t,\mathbf{r},\mathbf{k}}(d\omega), \end{aligned} \quad (134)$$

where we have used the Markov property (114) as well as the mutual independence among the subfamilies inherited in Rule 5.

Finally, by the definition (118), we have

$$\int_{\Omega_i} \mu_A(\omega_i) \Pi_{t+\tau_0, \mathbf{r}_i, \mathbf{k}_i}(\mathrm{d}\omega_i) = \psi(\mathbf{r}_i, \mathbf{k}_i, t + \tau_0), \quad i = 1, 2, 3. \quad (135)$$

Then the first right-hand-side term of Eq. (134) becomes

$$\begin{aligned} \int_{E^c} \zeta(\mathbf{r}(\tau_0)) \psi(\mathbf{r}_1, \mathbf{k}_1, t + \tau_0) \Pi_{t, \mathbf{r}, \mathbf{k}}(\mathrm{d}\omega) &= \int_t^T \mathrm{d}t_1 \mathrm{e}^{-\int_t^{t_1} \gamma(\mathbf{r}(s-t)) \mathrm{d}s} \\ &\times \int_{\mathbb{R}^d} \mathrm{d}\mathbf{r}_1 \int_{\mathcal{K}} \mathrm{d}\mathbf{k}_1 \{V_w^-(\mathbf{r}(t_1 - t), \mathbf{k} - \mathbf{k}_1) \cdot \delta(\mathbf{r}(t_1 - t) - \mathbf{r}_1)\} \psi(\mathbf{r}_1, \mathbf{k}_1, t_1), \end{aligned} \quad (136)$$

where we have let  $t + \tau_0 \rightarrow t_1$  and used Eqs. (99) and (109). The other two right-hand-side term of Eq. (134) terms can be treated in a similar way, and putting them together recovers the second right-hand-side term of Eq. (77). We complete the proof.  $\square$

For the adjoint equation (77), we have proven the existence of the solution, while its uniqueness can be deduced by the Fredholm alternative. It remains to validate the convergence of Eq. (104). To this end, we let  $\nu$  be a probability measure on the Borel sets of  $\mathbb{R}^d \times \mathcal{K}$  with the density  $f_I(\mathbf{r}, \mathbf{k}, t_l)$ , then it yields a unique product measure  $\nu \otimes \Pi_{t, \mathbf{r}, \mathbf{k}}$ . Consequently, from Eq. (92), we obtain

$$\begin{aligned} \langle A \rangle_{t_{l+1}} &\approx \iint_{\mathbb{R}^d \times \mathcal{K}} \varphi(\mathbf{r}, \mathbf{k}, t_l) \cdot \frac{f_S(\mathbf{r}, \mathbf{k}, t_l)}{f_I(\mathbf{r}, \mathbf{k}, t_l)} \cdot f_I(\mathbf{r}, \mathbf{k}, t_l) \mathrm{d}\mathbf{r} \mathrm{d}\mathbf{k} \\ &= \iint_{\mathbb{R}^d \times \mathcal{K}} \left[ \int_{\Omega} \mu_A(\omega) \Pi_{t_l, \mathbf{r}, \mathbf{k}}(\mathrm{d}\omega) \right] \cdot \frac{f_S(\mathbf{r}, \mathbf{k}, t_l)}{f_I(\mathbf{r}, \mathbf{k}, t_l)} \cdot \nu(\mathrm{d}\mathbf{r} \times \mathrm{d}\mathbf{k}) \\ &= \iint_{\mathbb{R}^d \times \mathcal{K} \times \Omega} \mu_A(\omega) \cdot \frac{f_S(\mathbf{r}, \mathbf{k}, t_l)}{f_I(\mathbf{r}, \mathbf{k}, t_l)} \cdot \nu \otimes \Pi_{t_l, \mathbf{r}, \mathbf{k}}(\mathrm{d}\mathbf{r} \times \mathrm{d}\mathbf{k} \times \mathrm{d}\omega) \\ &\approx \sum_{\alpha} \mu_A(\omega_{\alpha}) \cdot w_{\alpha}(t_l) = \sum_{\alpha} \sum_{i \in \mathcal{E}(\omega_{\alpha})} \phi_{i, \alpha} \cdot A(\mathbf{r}_{i, \alpha}, \mathbf{k}_{i, \alpha}) \cdot w_{\alpha}(t_l), \end{aligned} \quad (137)$$

and thus fully recover the approximation (104) (implying both  $\mathcal{E}_{\alpha}$  and  $\mathcal{E}(\omega_{\alpha})$  denote the same set), where Theorem 4 and Eq. (117) are applied in the second and fourth lines, respectively. Here  $N_{\alpha}$  independent samples  $(\mathbf{r}_{\alpha}, \mathbf{k}_{\alpha}, \omega_{\alpha})$  are generated from the product measure  $\nu \otimes \Pi_{t_l, \mathbf{r}, \mathbf{k}}$ , and  $\omega_{\alpha}$  stands for the family history with ancestor at time  $t_l$  at state  $(\mathbf{r}_{\alpha}, \mathbf{k}_{\alpha})$ . From the  $L^1$ -convergence of  $\mu_A$  in Eq. (130) and the strong law of large number in Eq. (91), we know that the approximation (104) converges almost surely when  $N_{\alpha} \rightarrow \infty$ , thus give a positive answer for Question 1.

In particular, we set  $t = 0$ ,  $\phi = 1$ ,  $A(\mathbf{r}, \mathbf{k}) \equiv 1$ , and then it can be verified that  $\varphi(\mathbf{r}, \mathbf{k}, t) \equiv 1$  is the unique solution of Eq. (77) using the mass conservation (19). By Theorem 4, the first moment of  $\mu_A$  also equals to 1, i.e.,

$$1 \equiv \varphi(\mathbf{r}, \mathbf{k}, 0) = \int_{\Omega} \mu_A(\omega) \cdot \Pi_{0, \mathbf{r}, \mathbf{k}}(\mathrm{d}\omega) = \int_{\Omega} \sum_{i \in \mathcal{E}(\omega)} \phi_i \cdot \Pi_{0, \mathbf{r}, \mathbf{k}}(\mathrm{d}\omega), \quad (138)$$

and then it further implies

$$\int_{\mathbb{R}^d} d\mathbf{x} \int_{\mathcal{K}} d\mathbf{k} f(\mathbf{x}, \mathbf{k}, T) = \langle A \rangle_T = \int_{\mathbb{R}^d} d\mathbf{r} \int_{\mathcal{K}} d\mathbf{k} f(\mathbf{r}, \mathbf{k}, 0), \quad \forall T \geq 0, \quad (139)$$

due to Eqs. (57) and (70), which is nothing but the mass conservation law (20). Furthermore, for such special case, we can show below that  $\sum_{i \in \mathcal{E}(\omega)} \phi_i = 1$  is almost sure for any family history  $\omega$ , not just the first moment as shown in Eq. (138). That is, the estimator (104) using finite number of super-particles is still able to preserve the mass conservation with probability 1, say,

$$\int_{\mathcal{R}^d \times \mathcal{K}} f(\mathbf{r}, \mathbf{k}, t_{l+1}) d\mathbf{r} d\mathbf{k} \approx \sum_{\alpha} \mu_A(\omega_{\alpha}) \cdot w_{\alpha}(t_l) = \sum_{\alpha} w_{\alpha}(t_l) = 1, \text{ a.s.} \quad (140)$$

**Theorem 5** (Mass conservation). *Suppose the weight of ancestor particle is  $\phi = 1$ . Then we have*

$$\Pr(E) = \int_{\Omega} 1_E(\omega) \Pi_{0, \mathbf{r}, \mathbf{k}}(d\omega) = 1, \quad (141)$$

where the event  $E$  is given by

$$E = \{\omega \in \Omega : \sum_{i \in \mathcal{E}(\omega)} \phi_i = 1\}. \quad (142)$$

*Proof.* Since  $Z(\omega, T - t)$  only takes odd values, it suffices to take

$$E_n = \{\omega \in \Omega : \sum_{i \in \mathcal{E}(\omega)} \phi_i = 1; Z(\omega, T - t) \leq 2n + 1\}, \quad (143)$$

$$E_n^* = \{\omega \in \Omega : Z(\omega, T - t) \leq 2n + 1\}, \quad (144)$$

and it is easy to see  $\Pr(E_0) = \Pr(E_0^*)$ . In the remaining part of the proof, we will omit  $\omega \in \Omega$  for brevity. Assume that the statement that  $\Pr(E_k) = \Pr(E_k^*)$  is true for  $0 \leq k \leq n, \forall t \in [0, T]$ . We show below by the mathematical induction that it still holds for  $k = n + 1$ .

From  $\omega = (Q_0; \omega_1; \omega_2; \omega_3)$ , it can be easily verified that

$$Z(\omega, T - t) = Z(\omega_1, T - t - \tau_0) + Z(\omega_2, T - t - \tau_0) + Z(\omega_3, T - t - \tau_0) \quad (145)$$

thus we have

$$Z(\omega_l, T - t - \tau_0) < Z(\omega, T - t), \quad \forall l \in \{1, 2, 3\}, \quad (146)$$

implying

$$E_{n+1}^* \subset \{Z(\omega_l, T - t - \tau_0) \leq 2n + 1\}, \quad \forall l \in \{1, 2, 3\}. \quad (147)$$

Furthermore, since

$$\sum_{i \in \mathcal{E}(\omega)} \phi_i = \phi(\mathbf{r}(\tau_0)) \cdot \left[ \sum_{i \in \mathcal{E}(\omega_1)} \phi_i - \sum_{i \in \mathcal{E}(\omega_2)} \phi_i \right] + \sum_{i \in \mathcal{E}(\omega_3)} \phi_i, \quad (148)$$

we obtain

$$\bigcap_{l=1}^3 \{ \sum_{i \in \mathcal{E}(\omega_l)} \phi_i = 1 \} \subset \{ \sum_{i \in \mathcal{E}(\omega)} \phi_i = 1 \}. \quad (149)$$

Combining Eqs. (147) and (149) with the conditionally independence of  $\omega_l$  yields

$$\begin{aligned} \frac{\Pr(E_{n+1})}{\Pr(E_{n+1}^*)} &\geq \Pr\left(\bigcap_{l=1}^3 \{ \sum_{i \in \mathcal{E}(\omega_l)} \phi_i = 1 \} \middle| E_{n+1}^*\right) = \prod_{l=1}^3 \Pr\left(\{ \sum_{i \in \mathcal{E}(\omega_l)} \phi_i = 1 \} \middle| E_{n+1}^*\right) \\ &= \prod_{l=1}^3 \Pr\left(\{ \sum_{i \in \mathcal{E}(\omega_l)} \phi_i = 1 \} \middle| \{Z(\omega_l, T - t - \tau_0) \leq 2n + 1\} \cap E_{n+1}^*\right) \\ &= 1, \end{aligned}$$

where the induction hypothesis is applied in the last line, and thus  $\Pr(E_{n+1}) \geq \Pr(E_{n+1}^*)$ . Accordingly, we have  $\Pr(E_{n+1}) = \Pr(E_{n+1}^*)$  for it is obvious that  $\Pr(E_{n+1}) \leq \Pr(E_{n+1}^*)$ .

Finally, according to the fact that  $E_0 \subset E_1 \subset \dots \subset E_n \subset E_{n+1} \dots \subset E$ , we have

$$\Pr(E) = \lim_{n \rightarrow +\infty} \Pr(E_n) = 1, \quad (150)$$

due to the monotone convergence theorem. Hence we complete the proof by setting  $t = 0$ .  $\square$

In the proof of Theorem 5, the latent assumption, namely, *two particles carrying the same weight but opposite sign must be generated in pair*, is required to conserve numerically the mass.

Now we turn to Question 2. For the constant auxiliary function  $\gamma(\mathbf{r}) \equiv \gamma_0$ , the random life-length  $\tau$  of a particle starting at time  $t$  is characterized by an exponential distribution

$$G(t') = \Pr(\tau < t' - t) = 1 - e^{-\gamma_0(t' - t)}, \quad t' \geq t. \quad (151)$$

In this case, the growth of particle number has been thoroughly studied in the literature and we are able to obtain a simple calculation formula of the particle number as shown in Theorem 6.

**Theorem 6.** *Suppose the family history  $\omega$  starts at  $t = 0$  and the constant auxiliary function  $\gamma(\mathbf{r}) \equiv \gamma_0$  is adopted. Then the expectation of the total number of frozen particles in time interval  $[0, T]$  is*

$$M(T) = e^{2\gamma_0 T}. \quad (152)$$

*Proof.* According to Theorem 15.1 of Chapter VI in [32], the expectation  $M(t')$  satisfies the following renewal integral equation

$$M(t') = 1 - G(t') + 3 \int_0^{t'} M(t' - u) dG(u), \quad M(0) = 1. \quad (153)$$

We substitute Eq. (151) into Eq. (153) and then can easily verify that  $M(t') = e^{2\gamma_0 t'}$  is the solution. The proof is finished.  $\square$

However, a direct estimate of number of frozen particles for a general auxiliary function  $\gamma(\mathbf{r})$  is still unknown in theory. In numerical simulations, Theorem 6 provides an upper bound of  $M(T)$  when the variable auxiliary function satisfies  $\gamma(\mathbf{r}) \leq \gamma_0$ . Whatever the auxiliary function is, it is clear that the particle number will grow exponentially. *To suppress the particle number, we can either decrease the parameter  $\gamma_0$  or choose a smaller final time  $T$ .* Theorem 6 also guides us on how to estimate the memory requirement for given  $\gamma_0$  and  $T$  in practice.

Finally, suppose we would like to evolve the branching particle system until the final time  $T$ . Usually, there are two ways. One is to evolve the system until each particle is frozen at the final time  $T$  in a single step. The other is to divide  $T$  into  $0 = t_0 < t_1 < \dots < t_{n-1} < t_n = T$  with  $t_n = n\Delta t$ , and then we evolve the system successively in  $n$  steps. However, the following theorem tells us that both produce the same  $M(T)$ .

**Theorem 7** (Theorem 11.1 of Chapter VI in [32]). *Suppose  $G(t) = 1 - e^{-\gamma_0 t}$ . Then  $Z(\omega, t)$  is a Markov branching process. In addition,  $Z(\omega, \Delta t), Z(\omega, 2\Delta t), \dots$  is a Galton-Watson process.*

We recall that for a Galton-Watson model, if  $M(\Delta t) = \beta$ , then  $M(n\Delta t) = \beta^n$ . From Eq. (152), we know that  $\beta = e^{2\gamma_0 \Delta t}$ , so that  $M(n\Delta t) = e^{2\gamma_0 T}$ . Therefore, we cannot expect to reduce the particle number by simply dividing  $T$  into several steps and evolve the particle system successively, which also manifests the indispensability of the resampling (or annihilation) procedure.

## 6 Numerical treatments

We turn to discuss the numerical aspects. The whole picture has been described in Section 5.2, so we only need to clarify several key treatments in numerical simulations. In this work, as an example, our numerical experiments focus on a one dimensional problem, where length, time and energy are measured in nanometer (nm), femtosecond (fs) and electron volt (eV), respectively. The potential function  $V(x)$  is chosen as the Gaussian barrier

$$V(x) = H_B \exp \left[ -\frac{(x - x_B)^2}{2} \right], \quad (154)$$

where  $H_B$  and  $x_B$  are the barrier height and the barrier center, respectively. From Eq. (21), we can readily obtain the explicit expression of corresponding Wigner kernel

$$V_w(x, k) = \frac{2H_B}{\hbar} \sqrt{\frac{2}{\pi}} e^{-2k^2} \sin(2k(x - x_B)). \quad (155)$$

### 6.1 Computing the normalization factor $\xi(x)$

For  $k$ -truncated Wigner equation, the normalization factor  $\xi(x)$  is given by

$$\xi(x) = \int_{2\kappa} V_w^+(x, k) dk. \quad (156)$$

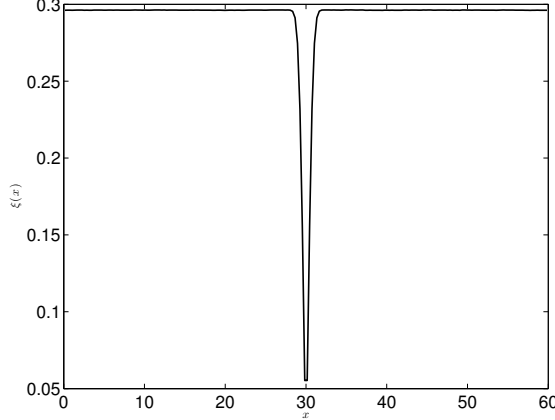


Figure 2: The normalization factor  $\xi(x)$  for the Gaussian barrier (154) with  $H_B = 0.3\text{eV}$  and  $x_B = 30\text{nm}$  is utilized in the  $k$ -truncated Wigner simulations.

In general, the calculation of  $\xi(x)$  and sampling from  $V_w^+(x, k)/\xi(x)$  can be realized simultaneously, say, we can calculate the normalization factor through sampling. In this case, we find that  $\sqrt{\frac{2}{\pi}}e^{-2k^2}$  in Eq. (155) is the probability density of the normal distribution  $\mathcal{N}(0, 1/2)$ , which provides an efficient way to calculate the integral. In actual simulations, the number of samples are chosen as  $2 \times 10^8$  for each  $x$ , and the numerical  $\xi(x)$  is shown in Fig. 2 for  $H_B = 0.3\text{eV}$  and  $x_B = 30\text{nm}$ . We find there that the normalization factor has a sharp decrease around  $x = 30$ , whereas it is very flat outside the neighborhood of  $x = 30$ .

For the  $y$ -truncated model, the computation of  $\xi(x)$  is relatively easier since it only involves the summation of discrete samples, while the modified Wigner kernel  $\tilde{V}_w(x, k)$  in Eq. (27) can be approximated by the rectangular formula. A similar profile to that shown in Fig. 2 is also observed.

## 6.2 Choosing the auxiliary function $\gamma(\mathbf{r})$

To randomly choose the lifetime of each particle, we need to choose the auxiliary function  $\gamma(\mathbf{r})$ . The original signed particle Wigner Monte Carlo method employs [22, 28]

$$\gamma(\mathbf{r}) = \xi(\mathbf{r}) = \int_{2\mathcal{K}} V_w^+(\mathbf{r}, \mathbf{k}) d\mathbf{k}, \quad (157)$$

with which the cumulative weight of particle  $i$  defined in Eq. (116) can only take  $\pm 1$ , i.e.,  $\phi_i \in \{-1, 1\}$ . This choice may facilitate the understanding of the particle model. However, we will show below that it may not be a good choice for numerical applications.

The main problem lies in the generation of a random life-length for each particle. Recall that the lifetime of each particle, initially at time  $t_0$ , satisfies

$$\tau \propto \left. \frac{d\mathcal{G}(t'; \mathbf{r}, t_0)}{dt'} \right|_{t'=t_0+\tau}. \quad (158)$$



To draw samples from such a distribution, we can generate a random number  $R$  from  $U[0, 1]$  such that

$$R = \mathcal{G}(t_0 + \tau; \mathbf{r}, t_0), \quad (159)$$

and then a simple calculation yields

$$\int_{t_0}^{t_0+\tau} \gamma(\mathbf{r}(s - t_0)) ds = -\ln(1 - R). \quad (160)$$

However, it is entirely not trivial to solve Eq. (160) for  $\tau$ . To this end, we always have to use an approximation like [22, 28]

$$\gamma(\mathbf{r}(s - t_0)) \approx \gamma(\mathbf{r}), \quad (161)$$

and thus

$$\tau \approx -\frac{\ln(1 - R)}{\gamma(\mathbf{r})}. \quad (162)$$

Usually, the approximation (161) is reasonable when  $\gamma(\mathbf{r}) = \xi(\mathbf{r})$  is very flat. But, for example, around the neighborhood of  $x = 30\text{nm}$  as shown in Fig. 2, such approximation may be too rough to be used and will give rise to additional numerical errors. By contrast, when choosing the constant auxiliary function  $\gamma(\mathbf{r}) \equiv \gamma_0$ , the life-length  $\tau$  of each particle turns out to be

$$\tau = -\frac{\ln(1 - R)}{\gamma_0}. \quad (163)$$

Meanwhile, it is also required that

$$\gamma_0 \geq \check{\xi} := \max_{\mathbf{r}} \xi(\mathbf{r}) \quad (164)$$

to ensure the boundedness of the cumulative weights (see Definition 4) as well as the  $L^1$ -convergence of  $\mu_A$  in Eq. (130).

### 6.3 Sampling in the continuous $k$ -space

The sampling in the discrete  $k$ -space is relatively simple, so we only focus on the sampling in the continuous  $k$ -space here. For the one-dimensional Gaussian barrier test, it can be achieved by the rejection sampling for we have the following estimate

$$V_w^+(x, k) \leq \frac{2H}{\hbar} h(k) \quad \text{and} \quad h(k) = \sqrt{\frac{2}{\pi}} e^{-2k^2}, \quad (165)$$

from Eq. (155). Here  $h(k)$  is nothing but the normal probability density. We apply the following procedure:

1. Draw a sample  $k$  from  $h(k)$  and compute the ratio

$$\alpha = \frac{\hbar}{2H} \frac{V_w^+(x, k)}{h(k)} \leq 1;$$

2. Generate a random number  $R$  from  $U[0, 1]$ . If  $R < \alpha$ , accept  $k$ ; otherwise, reject it and go back to the above step.

In this manner, the accepted samples will follow the target distribution  $V_w^+(x, k)/\xi(x)$ .

For high dimensional problems, the direct rejection sampling is not very efficient. So we need to resort to the Metropolis sampling or the Gibbs sampling and use a Markov chain to approximate the target distribution.

## 6.4 Resampling

As stated in Theorem 6, the particle number in the branching process will grow exponentially and may soon exceed the computational capacity. For example, when we draw  $\mathcal{O}(N_\alpha)$  samples according to the instrumental distribution  $f_I(\mathbf{r}, \mathbf{k}, t_l)$ , then the number of frozen particles at  $t_{l+1}$  is about  $\mathcal{O}(N_\alpha \cdot e^{2\gamma_0(t_{l+1}-t_l)})$ . However, after applying the resampling procedure, we only need to record the updated instrumental distribution  $f_I(\mathbf{r}, \mathbf{k}, t_{l+1})$  and draw  $\mathcal{O}(N_\alpha)$  new samples from it, without storing  $\mathcal{O}(N_\alpha \cdot e^{2\gamma_0(t_{l+1}-t_l)})$  super-particles. In this way, the resampling procedure sharply reduces the memory requirement for the data storage.

## 7 Numerical experiments

We now report a detailed description of numerical experiments performed for simulating the interaction dynamics of one-dimensional one-body Gaussian wavepacket with the Gaussian barrier potential (154). By setting the SEM solution with a fine mesh as the reference like we did in [23], we will compare the performance of the  $k$ -truncated (see Eq. (16), the model parameter is  $\Delta y$ ) and  $y$ -truncated (see Eq. (30), the model parameter is  $\Delta k$ ) branching particle models, both of which can be regarded as approximations of the same Wigner equation in the unbounded domain. Comparable results are expected on the same footing because both Gaussian wavepacket and Gaussian barrier possess a very nice localized structure. It should be noted that the results for the  $k$ -truncated Wigner branching process are reported here for the first time. Moreover, we want to verify the theoretical predictions as we discussed earlier, such as the effect of constant  $\gamma_0$ , the increasing behavior of the particle number, as well as the effect of the time step and the annihilation frequency.

We employ the relative  $L^2$  error to study the accuracy. Let  $f^{\text{ref}}(x, k, t)$  denote the reference Wigner function (wf) which could be the exact solution or the numerical solution on a relatively fine mesh, and  $f^{\text{num}}(x, k, t)$  the numerical solution. Then, the relative errors are written as

$$\text{err}_{wf}(t) = \left( \frac{\int_{\mathcal{X} \times \mathcal{K}} (\Delta f(x, k, t))^2 dx dk}{\int_{\mathcal{X} \times \mathcal{K}} (f^{\text{ref}}(x, k, t))^2 dx dk} \right)^{\frac{1}{2}}, \quad (166)$$

where  $\Delta f(x, k, t) = |f^{\text{num}}(x, k, t) - f^{\text{ref}}(x, k, t)|$ , and the integrals above are evaluated

using a simple rectangular rule over a uniform mesh

$$\begin{aligned} x_i &= x_{min} + (i - 1/2)\Delta x, \quad \Delta x = \frac{x_{max} - x_{min}}{200}, \quad i = 1, 2, \dots, 200, \\ k_j &= k_{min} + (j - 1)\Delta k, \quad \Delta k = \frac{k_{max} - k_{min}}{400}, \quad j = 1, 2, \dots, 400. \end{aligned} \quad (167)$$

In order to obtain a more complete view of the accuracy, we also measure corresponding relative errors for physical quantities, e.g. the spatial marginal (sm) probability distribution and the momental marginal (mm) probability distribution in a similar way, denoted by  $\text{err}_{sm}(t)$  and  $\text{err}_{mm}(t)$ , respectively. For the  $k$ -truncated branching particle model, we set the model parameter  $\Delta y = 0.6\text{nm}$  and thus the computational domain in the  $k$ -space  $\mathcal{K} = [k_{min}, k_{max}] = [-\pi/\Delta y, \pi/\Delta y] \approx [-5.2360\text{nm}^{-1}, 5.2360\text{nm}^{-1}]$  due to the constraint (23), and the mesh given in Eq. (167) is adopted to calculate the Wigner function. In order to put the comparison on the same footing, we use the same mesh for the  $y$ -truncated branching particle model, implying that the  $y$ -domain turns out to be  $\mathcal{Y} = [-\pi/\Delta k, \pi/\Delta k] = [-200\Delta y, 200\Delta y]$ . This  $y$ -domain is large enough to provide highly accurate calculation of the Wigner potential for Gaussian barriers with the height  $H = 0.3\text{eV}$  and  $1.3\text{eV}$  when using the Poisson summation formula [19]. For both models, we further set the  $x$ -domain to be  $\mathcal{X} = [x_{min}, x_{max}] = [0\text{nm}, 60\text{nm}]$ . The reference solutions by SEM are obtained with  $10 \times 20$  non-overlapping elements as well as a uniform mesh composed of  $31 \times 30$  collocation points on each element. The spectral accuracy of these reference solutions was well demonstrated in [19, 23] and more details can be also found there.

The motion of a Gaussian wavepacket [12, 19] is simulated to investigate the performance of the branching processes for time-dependent Wigner equation (7). The Gaussian wavepacket in the free space is

$$\begin{aligned} f(x, k, t) &= \frac{1}{\pi} \exp \left[ -\frac{(x - x_0 - v_0 t)^2}{2a^2(1 + \beta^2 t^2)} \right] \\ &\quad \times \exp \left\{ -2a^2(1 + \beta^2 t^2) \left[ (k - k_0) - \frac{\beta t(x - x_0 - v_0 t)}{2a^2(1 + \beta^2 t^2)} \right]^2 \right\}, \end{aligned} \quad (168)$$

where  $x_0$  is the center at  $t = 0$ ,  $a$  is the minimum position spread,  $v_0 = \frac{\hbar k_0}{m}$  is the average velocity, and  $\beta = \frac{\hbar}{2ma^2}$ . The kinetic energy of such Gaussian wavepacket is  $E_0 = \frac{\hbar^2 k_0^2}{2m}$ . Actually, the Gaussian wavepacket (168) is the analytical solution to the Wigner equation without a Wigner potential [12]. In the following numerical simulations, we take  $a = 2.825\text{nm}$ ,  $m = 0.0665m_e$  with  $m_e$  being the effective mass of electron,  $x_0 = 15\text{nm}$ ,  $k_0 = 0.7\text{nm}^{-1}$  (i.e.,  $E_0 \approx 0.2807\text{eV}$ ), and the final time  $t_{fin} = 20\text{fs}$ .

Once the Wigner branching process starts, the number of particles increases exponentially with time, thus necessary annihilation operations are required to make the simulation go on well, though they are not inherited in the branching process from the theoretical point of view. In this work, we do such annihilations at a

constant frequency, say  $1/T_A$ . That is, we divide equally the time interval  $[0, t_{fin}]$  into  $n_A$  subintervals with the partition being

$$0 = t^0 < t^1 < t^2 < \dots < t^{n_A} = t_{fin}, \quad n_A = t_{fin}/T_A.$$

The annihilations occur exactly at the time instant  $t^i$  for  $1 \leq i \leq n_A - 1$ , at which the particle number decreases significantly from  $\#_P^b(t^i)$  to  $\#_P^a(t^i)$ , where  $\#_P^b$  (resp.  $\#_P^a$ ) represents the particle number before (resp. after) the annihilation. For convenience, we denote the particle number at  $t^0$  and  $t^{n_A}$  by  $\#_P^a(t^0)$  and  $\#_P^b(t^{n_A})$ , respectively. In each time period  $[t^{i-1}, t^i]$ , the particle number increases from  $\#_P^a(t^{i-1})$  to  $\#_P^b(t^i)$  and corresponding multiple is denoted by

$$M_i = \#_P^b(t^i)/\#_P^a(t^{i-1}). \quad (169)$$

For the  $k$ -truncated Wigner branching particle model with constant auxiliary function  $\gamma(x) \equiv \gamma_0$ , it has been proved in Theorem 6 that such increasing multiple only depends on the time increment  $T_A$  and  $\gamma_0$ , which means the same increasing multiple exists for each time period, i.e.,  $M_i \equiv e^{2\gamma_0 T_A}$  for any  $i \in \{1, 2, \dots, n_A\}$ . We will verify this theoretical prediction in the following numerical simulations, during which the initial particle number is fixed to be  $\#_P^a(t^0) = 1641810$  as did in [23].

All the numerical results are obtained with our own serial Fortran implementations of the Wigner branching processes as well as SEM on the computing platform: Dell Poweredge R820 with  $4 \times$  Intel Xeon processor E5-4620 (2.2 GHz, 16 MB Cache, 7.2 GT/s QPI Speed, 8 Cores, 16 Threads) and 256GB memory. A fixed time step  $\Delta t$  is applied and then the total number of time steps becomes

$$n = t_{fin}/\Delta t.$$

When the branching process evolves from  $t_{j-1} = (j-1)\Delta t$  to  $t_j = j\Delta t$  for  $1 \leq j \leq n$ , particle offspring will be generated.

• **Experiment 1** To be convenient for comparison, we first take the same experiment as utilized before in [23], in which the barrier height is set to be  $H = 0.3\text{eV}$  so that the Gaussian wavepacket will be partially reflected. Such partial reflection is clearly shown in Fig. 3. Five groups of tests with different time steps and annihilation frequencies are performed and related data are displayed in Table 1, from which we are able to find several observations below concerning the accuracy.

- (1) The idea of choosing constant auxiliary function  $\gamma(x) \equiv \gamma_0$  works very well. As we expected, with the same  $\Delta t$  and  $T_A$ , the larger value  $\gamma_0$  takes, the more accurate solution we obtain, though more running time it spends. Interestingly, both accuracy and efficiency of the model with  $\gamma(x) = \xi(x)$  are very close to those of the model with  $\gamma(x) \equiv \check{\xi}$ , where  $\check{\xi} = \max_{x \in \mathcal{X}} \xi(x)$ . This also justifies the proposed mathematical framework, the algorithm of branching process as well as the implementation in some sense.
- (2) Highly frequent annihilation operations, e.g.,  $T_A = 0.1\text{fs}$ , destroy the accuracy, even larger constant auxiliary function cannot save it. But this does not mean

a low annihilation frequency should be appreciated. Actually, when using  $T_A = 4\text{fs}$ , the accuracy becomes worse than that using  $T_A = 1\text{fs}$  or  $2\text{fs}$ , which may be due to the accumulated numerical errors, such as the variance. That is, as we mentioned before, the annihilation adopted here is nothing but a kind of resampling to keep the mean value, and thus possibly suppresses some random noises.

- (3) While using the same annihilation frequency, say  $T_A = 1\text{fs}$ , smaller time step, e.g.,  $\Delta t = 0.008\text{fs}$ , cannot improve the accuracy, as predicted by Theorem 7. In fact, the accuracy with  $\Delta t = 0.008\text{fs}$  is almost identical to that with  $\Delta t = 1\text{fs}$ . But the former takes much more running time than the latter. Moreover, too small time steps will significantly reduce the probability of branching, which is crucial to capture the quantum information in stochastic Wigner simulations, so that nearly all particles do field-less travel in phase space. This point has been also mentioned in [23] when choosing the time step.

Next we focus on the efficiency. One of the main variables shaping the efficiency is the particle number. Since the same initial particle distribution is employed for all runs, we only need to consider the growth rate of particle number. Once choosing the constant auxiliary function  $\gamma_0$  and the annihilation frequency  $1/T_A$ , the increasing multiple of particle number can be exactly determined by  $e^{2\gamma_0 T_A}$  from Theorem 6, and the eighth column of Table 1 shows corresponding theoretical predictions. In our numerical simulations, within every annihilation period  $[t^{i-1}, t^i]$  with  $1 \leq i \leq n_A$ , we record the starting particle number  $\#_P^a(t^{i-1})$ , the ending particle number  $\#_P^b(t^i)$ , and the related growth rate  $M_i$  in Eq. (169). Let

$$\check{\#}_P^a = \max_{0 \leq i \leq n_A-1} \{\#_P^a(t^i)\}, \quad \check{\#}_P^b = \max_{1 \leq i \leq n_A} \{\#_P^b(t^i)\}, \quad \overline{M} = \frac{1}{n_A} \sum_{i=1}^{n_A} M_i.$$

Table 1 gives numerical values of above three quantities, see the fifth, sixth and seventh columns. According to Table 1, we can figure out the following facts on the efficiency.

- (1) Agreement between the mean value  $\overline{M}$  and the theoretical prediction  $e^{2\gamma_0 T_A}$  is readily seen in all situations. Actually, the growth rates in the first five annihilation periods, e.g. for  $T_A = 1\text{fs}$  and  $\gamma_0 = 3\xi$ , are 5.92, 5.87, 5.88, 5.89, and 5.88, all of which are almost identical to the mean value of 5.89. When  $T_A = 1, 2, 4\text{fs}$ , the former is a little less than the latter, because the particles moving outside the computational domain  $\mathcal{X} \times \mathcal{K}$  are not taken into account. Within each annihilation period, the maximum travel distance of particles can be calculated by

$$\frac{\hbar}{m} \cdot \max_{k \in \mathcal{K}} \{|k|\} \cdot T_A,$$

implying that, the larger value  $T_A$  is, the more particles move outside the domain. This explains the slight deviation between  $\overline{M}$  and  $e^{2\gamma_0 T_A}$  increases from almost zero to at most 1.33 as  $T_A$  increases from 0.1fs to 4fs. Moreover,

when  $T_A = 1\text{fs}$ , the increasing multiples for  $\Delta t = 0.008\text{fs}$  are identical to those for  $\Delta t = 1\text{fs}$ , i.e.,  $\bar{M}$  is independent of  $\Delta t$ , which has been also already predicted by the theoretical analysis. More details about the agreement of the growth rates of particle number with the theoretical prediction for  $T_A = 1\text{fs}$  and  $\Delta t = 0.008\text{fs}$  can be found in Fig. 4.

- (2) Not like using the constant auxiliary function, we do not have a simple calculation formula so far for the growth rate of particle number when using the variable auxiliary function (i.e., depending both on time and trajectories). However, we can still utilize the growth rate for the case of  $\gamma_0 = \check{\xi}$  to provide a close upper bound for the case of  $\gamma(x) = \xi(x)$ . As shown in the seventh column of Table 1, the variation of the mean growth rate between them is about 0, 0.03, 0.12 and 0.74 for  $T_A = 0.1\text{fs}$ ,  $1\text{fs}$ ,  $2\text{fs}$  and  $4\text{fs}$ , respectively. Fig. 4 further compares the curves of growth rate for  $T_A = 1\text{fs}$  and  $\Delta t = 0.008\text{fs}$  within four typical annihilation periods. By comparing with the Wigner functions shown in Fig. 3, we find that the closer to the center the Gaussian wavepacket lives, the larger the deviation between the curves for the constant and variable auxiliary functions becomes. Such deviation in accordance with the analysis of  $\xi(x)$  shown in Fig. 2 (see Section 6.1) validates the proposed mathematical theory again.
- (3) During the resampling (annihilation) procedure, the main objective is to reconstruct the Wigner distribution using less particles, which explores the cancellation of the weights with opposite signs, see Eq. (90). The sixth column of Table 1 tells us that the maximum particle numbers after resampling for  $T_A = 1, 2, 4\text{fs}$  are all around 3.00 million, implying that there should be a minimal requirement of particle number to achieve a comparable accuracy. Otherwise, the accuracy will decrease, for example, the values of  $\check{\#}_P^a$  for  $T_A = 0.1\text{fs}$  are around 2.55 million. Fig. 5 shows more clearly the typical history of  $\#_P^a(t)$ . We can find there that, no matter how huge the particle number before the annihilation  $\#_P^b(t)$  (which depends on both  $\gamma(x)$  and  $T_A$ ) is, the particle number after the annihilation  $\#_P^a(t)$  for the simulations with comparable accuracy exhibits almost the same behavior, which recovers and extends the so-called “bottom line” structure described in [23]. Such behavior may depend only on the oscillating structure of the Wigner function. On the other hand, highly frequent annihilations like  $T_A = 0.1\text{fs}$  destroy this bottom line structure and thus the accuracy, see Fig. 5(b), implying that there are not enough particles to capture the oscillating nature.

As we expected, all above observations can also be found in integrating the  $y$ -truncated Wigner branching model, and thus the detailed discussion is skipped here for saving the space. But many researchers in the literature are still working on the model, so we would also like to provide the running data in Table 2 for their possible reference.

• **Experiment 2** In this example, we increase the barrier height to  $H = 1.3\text{eV}$  so that the Gaussian wavepacket will be totally reflected, see Fig. 6. Such augment

of the barrier height implies that the growth rate of particle number now is about  $1.3/0.3 \approx 4.33$  times larger than that for Experiment 1, and thus it is more difficult to simulate accurately. Based on the observations in Experiment 1, we only test two groups of annihilation periods,  $T_A = 0.1, 1\text{fs}$ , using the  $k$ -truncated Wigner branching process. Table 3 summarizes the running data and confirms again that, the larger constant auxiliary function improves the accuracy, whereas the higher annihilation frequency destroys the accuracy. In order to get a more clear picture on this accuracy issue, we plot both spatial and momental probability distributions at different time instants  $t = 5, 20, 15, 20\text{fs}$  in Figs. 7 and 8 against the reference solutions by SEM. We can easily see there that, the loss of accuracy when using  $T_A = 0.1\text{fs}$  is mainly due to that there are not enough generated particles to capture the peaks reflecting off the barrier; while the increase of accuracy when using a larger constant auxiliary function, e.g.,  $\gamma_0 = 2\xi$ , comes from the smaller variation. Actually, similar phenomena also occur in Experiment 1.

## 8 Conclusion and discussion

In this work, we have established a sound mathematical framework for the Wigner branching process, which provides a probabilistic approach to the Wigner equation in theory, as well as yielding an efficient numerical method. We introduced a branching particle system associated with an exit system to depict the Wigner branching process in picturesque language, and exploited its theoretical background, namely, the solution of the Wigner equation or its adjoint equation is equivalent to the first moment of a stochastic branching process. Furthermore, when the life-length of super-particles is characterized by an exponential distribution with a constant parameter  $\gamma_0$ , we showed that the growth rate of particle number is expected to be  $e^{2\gamma_0 t}$  for a given time  $t$ , thereby providing a simple but rather reliable criterion to suppress the particle number in the simulations. Through typical numerical experiments, we demonstrated the feasibility of sampling in the continuous  $k$ -space, that also validates the  $k$ -truncated Wigner branching process, as well as the numerical accuracy of the proposed algorithms.

We would like to discuss the following topics in our future work.

- So far we have restricted our discussion on the first moment of the stochastic branching process, while the second moment is also very important as it is related to the variance, that also characterizes the numerical accuracy. In order to suppress the random noise more efficiently, it is necessary to thoroughly analyze the variance of the Wigner branching process.
- We have found in the simulations that when the Wigner function becomes more oscillating in the phase space, it requires more super-particles to capture the oscillating structure. Therefore, we would like to discuss the sophisticated techniques to adjust the distribution of particles adaptively, aiming at striking a balance between accuracy and efficiency.

- Moreover, we are urged to use the Wigner branching process to study many-body quantum systems, e.g., the Coulomb system where the Hamiltonian is given by the Hartree approximation. We expect to combine several advanced statistical techniques, such as an efficient Gibbs sampling and high dimensional clustering, in simulating the fully quantum many-body dynamics.

## Acknowledgement

This research was supported by grants from the National Natural Science Foundation of China (Nos. 11471025, 91330110, 11421101). The authors are grateful to the useful discussions with Zhenzhu Chen, Mihail Nedjalkov and Jean Michel Sellier on the signed particle Monte Carlo method for the  $y$ -truncated Wigner equation.

## References

- [1] J. L. Doob. *Classical Potential Theory and Its Probabilistic Counterpart*. Springer-Verlag, Berlin, reprint edition, 2001.
- [2] E. B. Dynkin. *Diffusions, Superdiffusions and Partial Differential Equations*. American Mathematical Society, 2002.
- [3] M. Nedjalkov and P. Vitinov. Application of the iteration approach to the ensemble Monte Carlo technique. *Solid-State Electron.*, 33:407–410, 1990.
- [4] C. Yan, W. Cai, and X. Zeng. A parallel method for solving Laplace equations with Dirichlet data using local boundary integral equations and random walks. *SIAM J. Sci. Comput.*, 35:B868–B889, 2013.
- [5] M. Hairer and J. Weare. Improved diffusion Monte Carlo. *Commun. Pure Appl. Math.*, 67:1995–2021, 2014.
- [6] E. Wigner. On the quantum corrections for thermodynamic equilibrium. *Phys. Rev.*, 40:749–759, 1932.
- [7] V. I. Tatarskiĭ. The Wigner representation of quantum mechanics. *Sov. Phys. Usp.*, 26:311–327, 1983.
- [8] W. H. Zurek. Decoherence and the transition from quantum to classical. *Phys. Today*, October:36–44, 1991.
- [9] C. Jacoboni and P. Bordone. The Wigner-function approach to non-equilibrium electron transport. *Rep. Prog. Phys.*, 67:1033–1071, 2004.
- [10] N. C. Dias and J. N. Prata. Admissible states in quantum phase space. *Ann. Phys.*, 313:110–146, 2004.



- [11] P. A. Markowich, C. A. Ringhofer, and C. Schmeiser. *Semiconductor Equations*. Springer-Verlag, Wien-New York, 1990.
- [12] B. A. Biegel. *Quantum Electronic Device Simulation*. PhD thesis, Stanford University, 1997.
- [13] R. Balescu. *Equilibrium and Nonequilibrium Statistical Mechanics*. John Wiley & Sons, New York, 1975.
- [14] W. P. Schleich. *Quantum Optics in Phase Space*. Wiley-VCH, Berlin, 2011.
- [15] J. M. Sellier, M. Nedjalkov, and I. Dimov. An introduction to applied quantum mechanics in the Wigner Monte Carlo formalism. *Phys. Rep.*, 577:1–34, 2015.
- [16] U. Leonhardt. *Measuring the Quantum State of Light*. Cambridge University Press, New York, 1997.
- [17] D. Leibfried, T. Pfau, and C. Monroe. Shadows and mirrors: Reconstructing quantum states of atom motion. *Phys. Today*, April:22–28, 1998.
- [18] C. Zachos. Deformation quantization: quantum mechanics lives and works in phase-space. *Int. J. Mod. Phys. A*, 17:297–316, 2002.
- [19] S. Shao, T. Lu, and W. Cai. Adaptive conservative cell average spectral element methods for transient Wigner equation in quantum transport. *Commun. Comput. Phys.*, 9:711–739, 2011.
- [20] Y. Xiong, Z. Chen, and S. Shao. An advective-spectral-mixed method for time-dependent many-body Wigner simulations. *Submitted*, 2015 [*arXiv:1602.08853*].
- [21] D. Querlioz and P. Dollfus. *The Wigner Monte Carlo Method for Nanoelectronic Devices: A Particle Description of Quantum Transport and Decoherence*. Wiley-ISTE, London, 2010.
- [22] J. M. Sellier, M. Nedjalkov, I. Dimov, and S. Selberherr. A benchmark study of the Wigner Monte-Carlo method. *Monte Carlo Methods Appl.*, 20:43–51, 2014.
- [23] S. Shao and J. M. Sellier. Comparison of deterministic and stochastic methods for time-dependent Wigner simulations. *J. Comput. Phys.*, 300:167–185, 2015.
- [24] L. Shifren and D. K. Ferry. Particle Monte Carlo simulation of Wigner function tunneling. *Phys. Lett. A*, 285:217–221, 2001.
- [25] L. Shifren and D. K. Ferry. A wigner function based ensemble monte carlo approach for accurate incorporation of quantum effects in device simulation. *J. Comput. Electron.*, 1:55–58, 2002.
- [26] L. Shifren, C. Ringhofer, and D. K. Ferry. A Wigner function-based quantum ensemble Monte Carlo study of a resonant tunneling diode. *IEEE Trans. Electron Devices*, 50:769–773, 2003.

- [27] M. Nedjalkov, H. Kosina, S. Selberherr, C. Ringhofer, and D. K. Ferry. Unified particle approach to Wigner-Boltzmann transport in small semiconductor devices. *Phys. Rev. B*, 70:115319, 2004.
- [28] M. Nedjalkov, P. Schwaha, S. Selberherr, J. M. Sellier, and D. Vasileska. Wigner quasi-particle attributes – An asymptotic perspective. *Appl. Phys. Lett.*, 102:163113, 2013.
- [29] H. Jiang, W. Cai, and R. Tsu. Accuracy of the Frensley inflow boundary condition for Wigner equations in simulating resonant tunneling diodes. *J. Comput. Phys.*, 230:2031–2044, 2011.
- [30] A. Pazy. *Semigroups of Linear Operators and Applications to Partial Differential Equations*. Springer-Verlag, New York, 1983.
- [31] I. Dimov, M. Nedjalkov, J. M. Sellier, and S. Selberherr. Boundary conditions and the Wigner equation solution. *J. Comput. Electron.*, 14:859–863, 2015.
- [32] T. E. Harris. *The Theory of Branching Processes*. Springer-Verlag, Berlin, 1963.
- [33] O. Kallenberg. *Foundations of Modern Probability*. Springer, New York, second edition, 2002.
- [34] R. Kress. *Linear Integral Equations*. Springer, New York, third edition, 2014.

Table 1: Partial reflection: Numerical data for the  $k$ -truncated Wigner branching particle model. The errors in the second, third and fourth columns are calculated at the final time  $t_{fin} = 20\text{fs}$ . The particle numbers in the fifth and sixth columns and the running CPU time in the last column are measured in million and minutes, respectively. While using constant auxiliary function  $\gamma(x) \equiv \gamma_0$  the increasing multiple of particle number within an annihilation period is  $e^{2\gamma_0 T_A}$ . Three kinds of constant auxiliary functions,  $\gamma_0 = \check{\xi}, 2\check{\xi}, 3\check{\xi}$ , are tested, where  $\check{\xi} = \max_{x \in \mathcal{X}} \{\xi(x)\} \approx 2.96\text{E-}01$ .

$\gamma(x)$	$\text{err}_{wf}$	$\text{err}_{sm}$	$\text{err}_{mm}$	$\check{\#}_P^b$	$\check{\#}_P^a$	$\overline{M}$	$e^{2\gamma_0 T_A}$	Time
$\Delta t = 0.008\text{fs}, T_A = 1\text{fs}$								
$\xi(x)$	9.08E-02	3.08E-02	3.20E-02	5.34	3.02	1.77	–	286.28
$\check{\xi}$	9.01E-02	3.16E-02	3.05E-02	5.44	3.02	1.80	1.81	291.45
$2\check{\xi}$	7.95E-02	2.74E-02	2.46E-02	9.62	2.95	3.26	3.27	297.72
$3\check{\xi}$	7.51E-02	2.52E-02	1.97E-02	17.25	2.93	5.89	5.91	314.83
$\Delta t = 1\text{fs}, T_A = 1\text{fs}$								
$\xi(x)$	9.25E-02	3.21E-02	3.31E-02	5.35	3.02	1.77	–	3.38
$\check{\xi}$	8.98E-02	3.32E-02	2.73E-02	5.44	3.02	1.80	1.81	3.37
$2\check{\xi}$	7.94E-02	2.68E-02	2.21E-02	9.61	2.95	3.26	3.27	4.57
$3\check{\xi}$	7.55E-02	2.51E-02	1.99E-02	17.26	2.93	5.89	5.91	6.55
$\Delta t = 2\text{fs}, T_A = 2\text{fs}$								
$\xi(x)$	9.43E-02	3.18E-02	3.75E-02	9.72	3.12	3.13	–	2.22
$\check{\xi}$	9.00E-02	3.45E-02	3.43E-02	10.07	3.10	3.25	3.27	2.95
$2\check{\xi}$	6.32E-02	2.70E-02	2.36E-02	31.62	2.98	10.62	10.68	5.50
$3\check{\xi}$	5.48E-02	2.45E-02	2.30E-02	102.25	2.94	34.71	34.88	14.63
$\Delta t = 4\text{fs}, T_A = 4\text{fs}$								
$\xi(x)$	1.39E-01	4.63E-02	4.66E-02	30.69	3.26	9.72	–	2.25
$\check{\xi}$	1.27E-01	4.93E-02	4.74E-02	33.19	3.21	10.46	10.68	2.63
$2\check{\xi}$	6.69E-02	2.83E-02	2.79E-02	326.99	2.92	112.65	113.98	25.10
$\Delta t = 0.1\text{fs}, T_A = 0.1\text{fs}$								
$\xi(x)$	2.86E-01	8.12E-02	6.82E-02	2.73	2.58	1.06	–	23.67
$\check{\xi}$	2.87E-01	8.02E-02	6.53E-02	2.73	2.57	1.06	1.06	23.82
$2\check{\xi}$	2.84E-01	8.01E-02	6.61E-02	2.87	2.55	1.13	1.13	24.07
$3\check{\xi}$	2.84E-01	8.10E-02	6.60E-02	3.04	2.55	1.19	1.19	24.83

Table 2: Partial reflection: Numerical data for the  $y$ -truncated Wigner branching particle model. Detailed explanations are referred to Table 1, except for  $\check{\xi} \approx 2.90\text{E-}01$  now.

$\gamma(x)$	$\text{err}_{wf}$	$\text{err}_{sm}$	$\text{err}_{mm}$	$\check{\#}_P^b$	$\check{\#}_P^a$	$\overline{M}$	$\mathfrak{e}^{2\gamma_0 T_A}$	Time
$\Delta t = 0.008\text{fs}, T_A = 1\text{fs}$								
$\xi(x)$	9.41E-02	2.66E-02	3.14E-02	5.13	2.93	1.75	–	290.22
$\check{\xi}$	9.32E-02	2.57E-02	2.87E-02	5.36	3.01	1.78	1.79	291.37
$2\check{\xi}$	8.22E-02	2.16E-02	2.18E-02	9.33	2.93	3.18	3.19	303.30
$3\check{\xi}$	7.86E-02	2.04E-02	1.85E-02	16.54	2.91	5.67	5.70	312.25
$\Delta t = 1\text{fs}, T_A = 1\text{fs}$								
$\xi(x)$	9.52E-02	3.24E-02	3.03E-02	5.14	2.94	1.75	–	3.07
$\check{\xi}$	9.56E-02	2.69E-02	2.97E-02	5.36	3.01	1.78	1.79	3.22
$2\check{\xi}$	8.34E-02	2.15E-02	2.05E-02	9.33	2.93	3.18	3.19	4.37
$3\check{\xi}$	7.95E-02	2.20E-02	1.94E-02	16.54	2.92	5.67	5.70	6.57
$\Delta t = 2\text{fs}, T_A = 2\text{fs}$								
$\xi(x)$	9.49E-02	2.73E-02	2.76E-02	9.22	3.03	3.06	–	2.22
$\check{\xi}$	8.99E-02	2.90E-02	3.03E-02	9.76	3.09	3.17	3.19	2.32
$2\check{\xi}$	6.47E-02	1.99E-02	1.96E-02	30.00	2.97	10.10	10.18	5.57
$3\check{\xi}$	5.56E-02	1.48E-02	1.55E-02	94.54	2.94	32.17	32.46	16.45
$\Delta t = 4\text{fs}, T_A = 4\text{fs}$								
$\xi(x)$	1.40E-01	4.46E-02	4.41E-02	28.35	3.16	9.27	–	2.92
$\check{\xi}$	1.30E-01	4.59E-02	4.37E-02	31.54	3.20	9.96	10.18	3.15
$2\check{\xi}$	6.81E-02	2.12E-02	2.01E-02	294.29	2.91	101.82	103.54	28.77
$\Delta t = 0.1\text{fs}, T_A = 0.1\text{fs}$								
$\xi(x)$	2.87E-01	7.57E-02	7.07E-02	2.64	2.49	1.06	–	23.53
$\check{\xi}$	2.88E-01	7.80E-02	6.91E-02	2.71	2.56	1.06	1.06	23.47
$2\check{\xi}$	2.88E-01	7.95E-02	7.19E-02	2.86	2.54	1.12	1.12	23.98
$3\check{\xi}$	2.86E-01	7.82E-02	7.08E-02	3.02	2.54	1.19	1.19	24.65

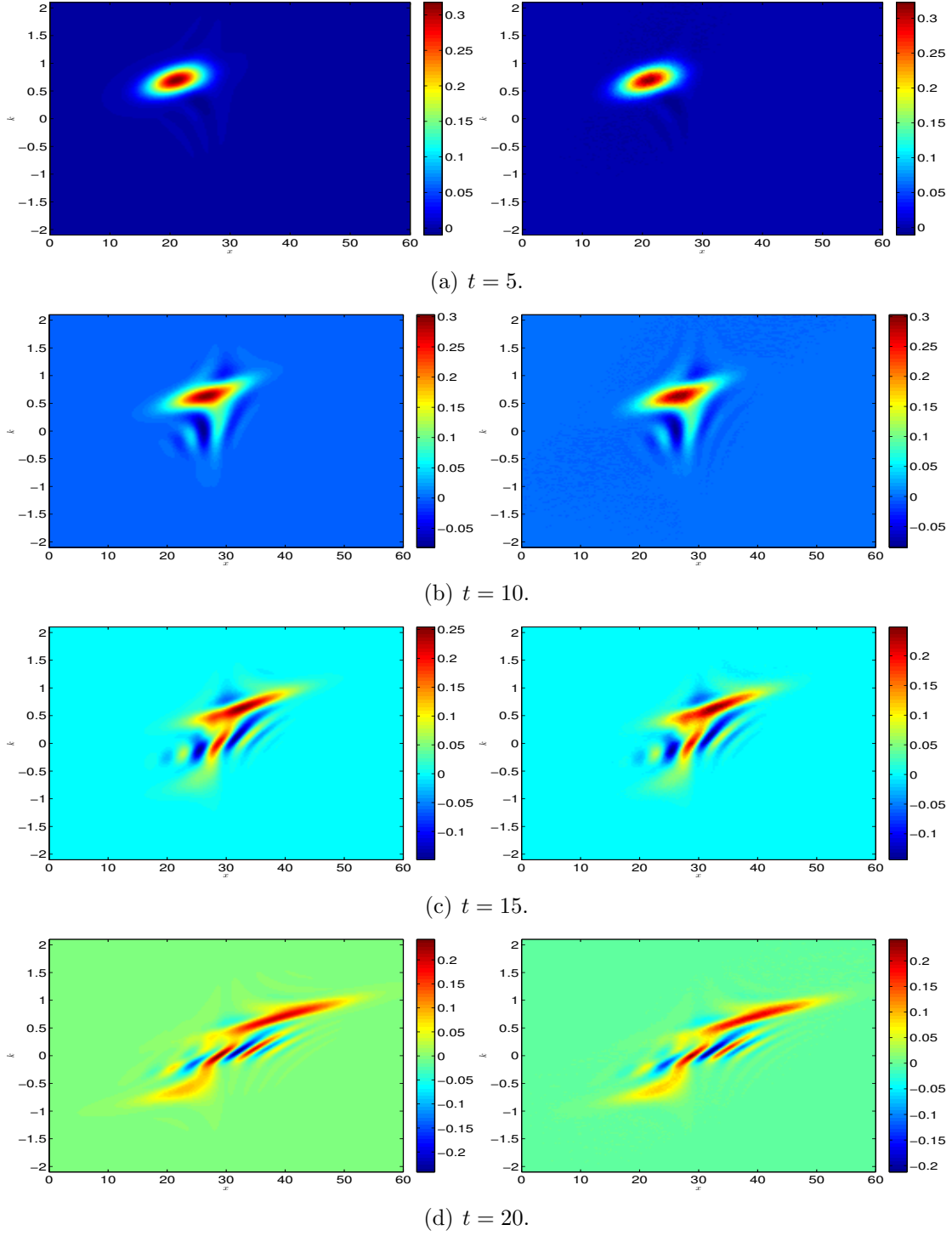


Figure 3: Partial reflection: Numerical Wigner functions at different time instants  $t = 5, 10, 15, 20$ fs. The reference solution by SEM is displayed in the left-hand-side column, while the right-hand-side column shows the numerical solution obtained from the  $k$ -truncated branching particle method with the auxiliary function  $\gamma(x) = 3\tilde{\xi}$  as well as  $\Delta t = 1$ fs and  $T_A = 1$ fs.

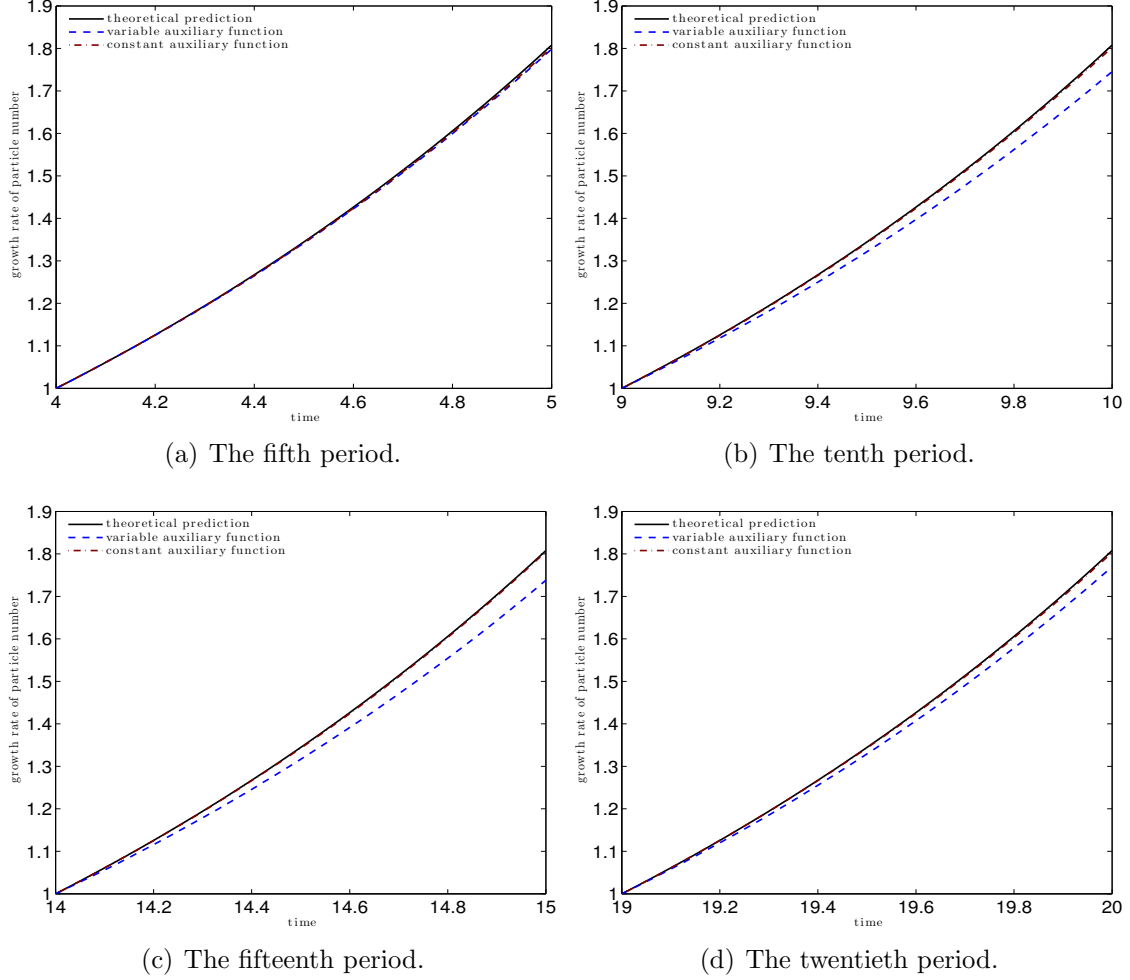


Figure 4: Partial reflection: Growth rates of particle number within different annihilation periods for the  $k$ -truncated branching particle method with  $\Delta t = 0.008\text{fs}$  and  $T_A = 1\text{fs}$ . The curve of theoretical prediction can be described analytically by  $e^{2\gamma_0 t}$  when using a constant auxiliary function  $\gamma_0$ . Here we set the constant auxiliary function  $\gamma_0 = \check{\xi}$  and the variable one  $\gamma(x) = \xi(x)$ .

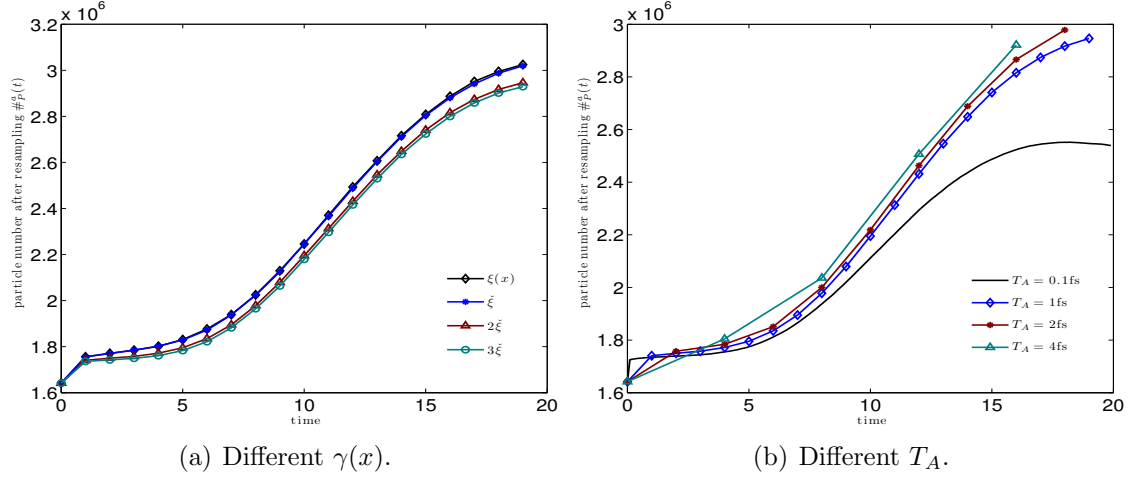


Figure 5: Partial reflection: Particle number after resampling (annihilation). The left plot shows the behavior for different auxiliary functions  $\gamma(x)$  with the same annihilation period  $T_A = 1$  fs. The right plot displays the behavior for different annihilation periods with the same constant auxiliary function  $\gamma_0 = 2\tilde{\xi}$ .

Table 3: Total reflection: Numerical data for the  $k$ -truncated Wigner branching particle model. Detailed explanations are referred to Table 1, except for  $\tilde{\xi} \approx 1.28$  here.

$\gamma(x)$	$\text{err}_{wf}$	$\text{err}_{sm}$	$\text{err}_{mm}$	$\tilde{\#}_P^b$	$\tilde{\#}_P^a$	$\overline{M}$	$e^{2\gamma_0 T_A}$	Time
$\Delta t = 1$ fs, $T_A = 1$ fs								
$\xi(x)$	2.6210E-01	7.1421E-02	7.6208E-02	48.63	3.95	12.45	—	11.33
$\tilde{\xi}$	2.5998E-01	6.7069E-02	8.4044E-02	49.58	3.94	12.71	13.04	12.48
$2\tilde{\xi}$	1.3034E-01	3.1041E-02	5.5122E-02	479.96	2.87	167.36	170.12	113.62
$\Delta t = 0.1$ fs, $T_A = 0.1$ fs								
$\xi(x)$	3.3899E-01	1.0171E-01	1.9413E-01	3.22	2.50	1.29	—	25.33
$\tilde{\xi}$	3.4201E-01	1.0674E-01	1.9785E-01	3.23	2.50	1.29	1.29	25.87
$2\tilde{\xi}$	3.3697E-01	1.0959E-01	1.9413E-01	4.05	2.43	1.67	1.67	28.98
$3\tilde{\xi}$	3.4011E-01	1.1157E-01	1.9734E-01	5.18	2.40	2.16	2.16	29.80

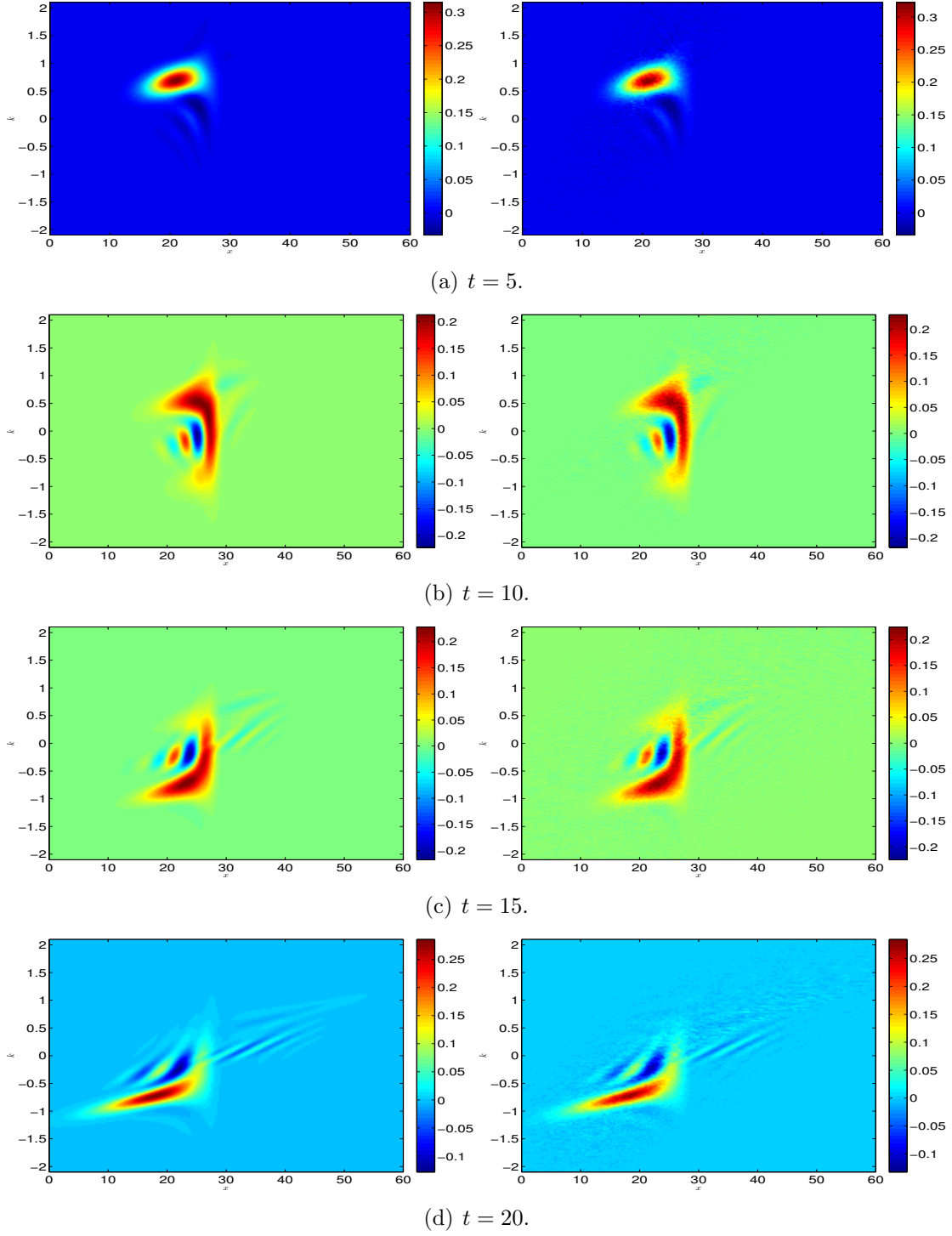


Figure 6: Total reflection: Numerical Wigner functions at different time instants  $t = 5, 20, 15, 20$ fs. The reference solution by SEM is displayed in the left-hand-side column, while the right-hand-side column shows the numerical solution obtained from the  $k$ -truncated branching particle method with the auxiliary function  $\gamma(x) = 2\tilde{\xi}$  as well as  $\Delta t = 1$ fs and  $T_A = 1$ fs.



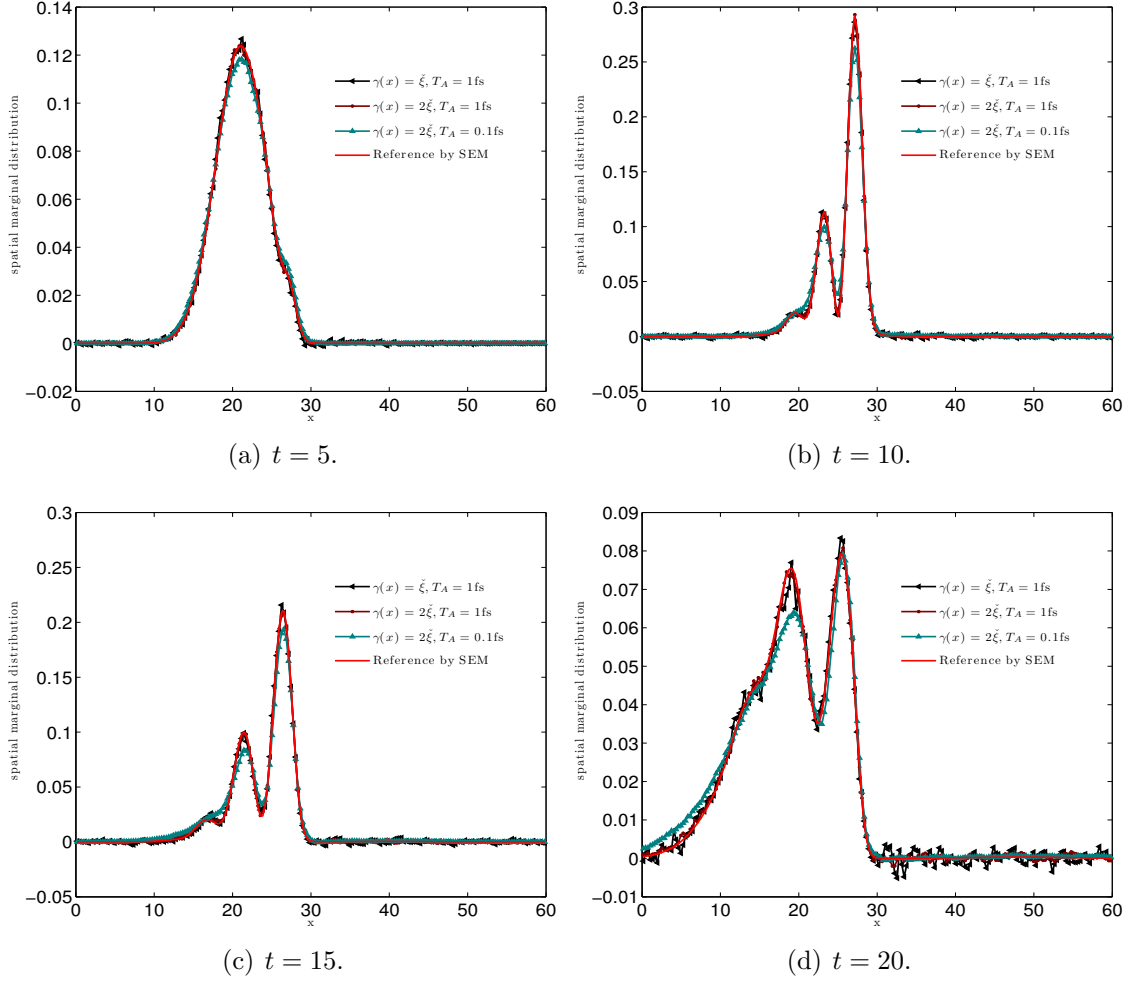


Figure 7: Total reflection: Spatial marginal probability distributions at different time instants  $t = 5, 20, 15, 20$ fs.

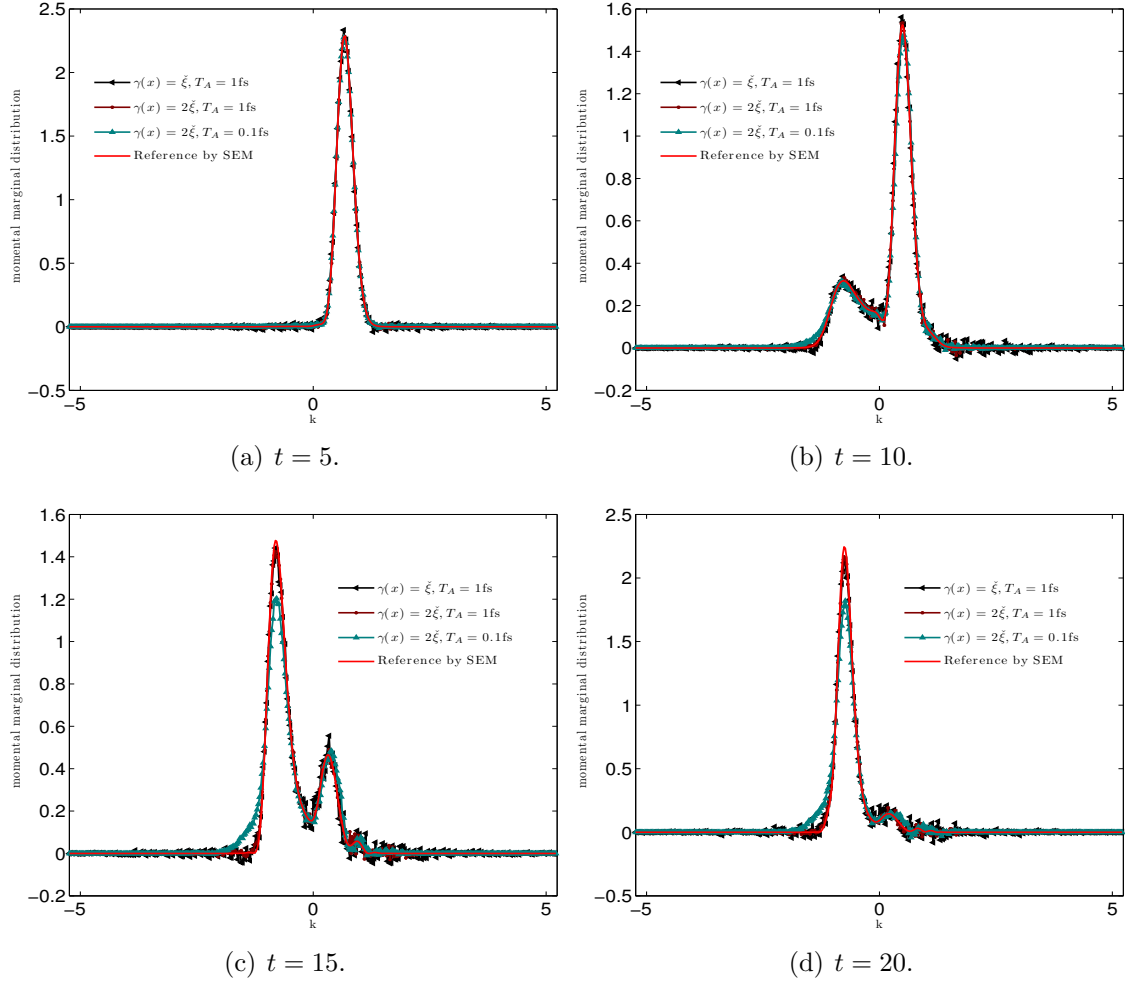


Figure 8: Total reflection: Momental marginal probability distributions at different time instants  $t = 5, 20, 15, 20$ fs.